High temperature crystal chemistry of K and Na fluor-richterites

Maryellen Cameron,[1] Shigeho sueno,[2] J. J. Papike,[3] and C. T. Prewitt

Department of Earth and Space Sciences
State University of New York
Stony Brook, New York 11794

Abstract

Crystal structure parameters have been determined for synthetic potassium richterite K(NaCa)Mg$_5$Si$_8$O$_{22}$F$_2$ at 24°, 400°, 600°, and 800°C, and synthetic sodium richterite Na(NaCa) Mg$_5$Si$_8$O$_{22}$F$_2$ at 24°, 400°, 600°, 800°, and 900°C. Anisotropic refinements in space group *I2/m* using 1150–1200 reflections resulted in *R* factors ranging from 0.034 to 0.063. The K atom in the A site of potassium richterite was refined at all temperatures using a half atom model with K randomly occupying two special positions (4*i*) within the (010) mirror plane. The Na atom in the A site of sodium richterite was refined using a quarter atom model in which Na randomly occupies four general positions (8*j*) off both the (010) mirror plane and the twofold axis parallel to *b*.

As observed in other high-temperature studies of silicate minerals, the polyhedra in these structures expand differentially. Over the temperature intervals studied, the tetrahedral distances remain statistically identical, but all other mean polyhedral distances increase significantly. Mean thermal expansion coefficients (MTEC) for mean bond lengths increase as follows: T1 = T2 ≪ M3 < M1 < M2 ≪ ^{VIII}M4 < ^{X}A (K richterite) and T1 = T2 ≪ M1 < M2 < M3 ≪ ^{VIII}M4 < ^{X}A (Na richterite). This differential polyhedral expansion is accompanied by straightening of the tetrahedral chains and by increased displacement of the double chains relative to each other. Expansion of three of the four M polyhedra in K richterite is slightly greater than for Na richterite, and the MTEC of its unit cell volume is larger (3.39 *vs.* 3.10/°C × 10^{-5}).

The behavior of the richterite structures at elevated temperatures is generally similar to that of tremolite. The MTEC's for structural and thermal parameters are often identical within three standard deviations. The largest difference among the three structures involves the coordination polyhedron about the A site, where the rate of expansion of the mean 10-coordinated A–O distance is significantly greater in the richterites than in tremolite.

Introduction

Phenomena such as exsolution, solid solution, and inter- and intracrystalline equilibria are of interest to geologists because they provide information on the crystallization and cooling histories of rocks. These phenomena typically occur at elevated temperatures and/or pressures in geologic environments, and until recently they were necessarily described on an atomic level in terms of room-temperature crystal structures. Within the last ten years, however, the structures of various rock-forming silicate minerals have been examined at temperatures up to 1050°C. Scores of refinements, on a limited number of crystals, have been published for olivines (*e.g.*, Brown and Prewitt, 1973; Hazen, 1976; Smyth and Hazen 1973; Lager and Meagher, 1978), feldspars (*e.g.*, Prewitt *et al.*, 1976; Winter *et al.*, 1979), pyroxenes (*e.g.*, Cameron *et al.*, 1973a; Sueno *et al.*, 1976), and amphiboles (*e.g.*, Sueno *et al.*, 1973). The crystals used in many of these high temperature studies have approximately end-member compositions, and thus the effects of increasing temperature on individual cations could be evaluated.

In this paper we describe the structural changes that occur in two synthetic fluor-richterites (KNaCaMg$_5$ Si$_8$O$_{22}$F$_2$ and NaNaCaMg$_5$Si$_8$O$_{22}$F$_2$) at a series of temperatures between 24° and 900°C. Our primary intention is to compare the behavior of an amphibole with a filled A site (richterite) to one with a vacant A site (tremolite; Sueno *et al.*, 1973). Richterites were selected for study

[1] Present address: School of Geology and Geophysics, University of Oklahoma, Norman, Oklahoma 73019.
[2] Present address: Institute of Geoscience, The University of Tsukuba, Ibaraki, 300-31, Japan.
[3] Present address: Institute for the Study of Mineral Deposits, South Dakota School of Mines and Technology, Rapid City, South Dakota 57701

because they have relatively simple chemistry (for amphiboles) and because good synthetic crystals were available. In addition to describing the room-temperature structures, we examine the systematics of thermal expansion of the two fluor-richterite structures and we compare their behavior at elevated temperatures to that of tremolite and diopside. The only other amphibole whose structure has been studied to high temperatures is primitive cummingtonite (Sueno *et al.*, 1972).

Experimental

The richterite crystals used in this study were synthesized by J. Stephen Huebner and are discussed by Huebner and Papike (1970). The crystals, both less than 100 μm in length, were mounted on quartz glass fibers and were oriented parallel to c^*. The special high-temperature cement used and the crystal heater are discussed in detail by Brown *et al.* (1973). The uncertainty in temperature for each refinement depends on the crystal temperature, but is approximately ±20°C (Brown *et al.*, 1973). The intensity data were collected in 1972, but the results presented in this paper were finalized in 1982.

Integrated intensities were measured at 24°, 400°, 600°, 800°C for K richterite and at 24°, 400°, 600°, 800°, 900°C for Na richterite with a PDP-15 computer-controlled Picker diffractometer with $MoK\alpha$ radiation monochromatized by a graphite crystal. The data were collected using an $\omega-2\theta$ scan (2°/minute) with five second background counts on both sides of each peak. Isotropic and anisotropic refinements were calculated for each data set in space group $I2/m$[4] using neutral atom scattering factors (Doyle and Turner, 1968), statistical weights, and the RFINE program of L. W. Finger. No absorption corrections were made because of the small size of the crystals and the small linear absorption coefficients for Mo radiation. The number of reflections used in each refinement and the final R factors for the anisotropic refinements are given in Table A1.[5] Observed structure factors and β_{ij}'s from the final cycle of each anisotropic refinement are listed in Table 1.[6] Other results of the refinements are reported as follows: Positional Parameters and Isotropic Temperature Factors (Table A2); Interatomic Distances in Tetrahedral Chains (Table A3); Interatomic Angles in Tetrahedral Chains (Table A4); Interatomic Distances in M Polyhedra of Richterites (Table A5); Interatomic Angles in M Polyhedra of Richterites (Table A6); Interatomic

Table 2. Models tested during refinement for the atom in the richterite A site

Model	24° K fluor-richterite	24° Na fluor-richterite
1. A atom constrained to special position 2*b* at intersection of mirror and twofold		
Isotropic R factor	0.077	0.065
B(Å²), A atom	4.3	9.4
2. A atom constrained to special position 4*i* within mirror (1/2 atom model)		
Isotropic R factor	0.054	0.052
B(Å²), A atom	2.2	4.8
3. A atom unconstrained, at general position 8*j* (1/4 atom model)		
Isotropic R factor	0.095	0.047
B(Å²), A atom	2.6	2.5

Distances in A Polyhedra of Richterites (Table A7); Magnitude and Orientation of Thermal Ellipsoids in K Richterite (Table A8); Magnitude and Orientation of Thermal Ellipsoids in Na Richterite (Table A9). No thermal corrections for interatomic distances were made because of the uncertainty in selecting an appropriate model that describes the thermal motion effect on bond distances.

During the initial refinements the Na and K atoms in the A sites were placed on the special position 2*b* at the intersection of the (010) mirror and the twofold axis parallel to *b*. Relatively high R factors and high temperature factors (Table 2) for the A cation indicated that a more suitable model for the A site was required. Accordingly, we also carried out refinements in which the single K or Na atom was replaced by two ½ atoms constrained to the (010) mirror plane (special position 4*i*) or by four 1/4 atoms at a general position (8*j*). For the K richterite, the lowest R factors were obtained with the ½ atom model and for the Na richterite, with the ¼ atom model (Table 2). In addition to lower R factors, the split-atom approximation also produced better errors associated with the positional parameters of the A cation. ΔF maps, which are discussed in a later section, are consistent with these models. We did not test models where the A cation was disordered along the twofold axis (special position 4*g*) for either structure. Such a model seemed unreasonable for the large K atom, a conclusion suported by the results of Hawthorne and Grundy (1978). In addition, refinements of Na richterite converged satisfactorily with the Na atom at the general position 8*j*, and indicated no systematic movement of Na to a position near the twofold axis.

Unit cell parameters were determined using 2θ values of 15-20 reflections measured on the Picker diffractometer. The 2θ values were refined using the PODEX2 program written by A. W. Sleight.[7] Cell parameters for

---

[4] Space group $I2/m$ was used rather than $C2/m$ to facilitate comparison with the $C2/c$ pyroxene structures. See Appendix VI in Cameron and Papike (1979) for a discussion of the relationship between the two space groups.

[5] Table numbers preceded by the letter "A" are located in the Appendix at the end of the paper. Tables without the prefix are included in the main text of the paper.

[6] To receive a copy of Table 1, order Document AM-83-230 from the Business Office, Mineralogical Society of America, 2000 Florida Ave., NW, Washington, D. C. 20009. Please remit $1.00 in advance for the microfiche.

[7] Central Research Dept., E. I. duPont de Nemours and Company, Wilmington, Delaware.
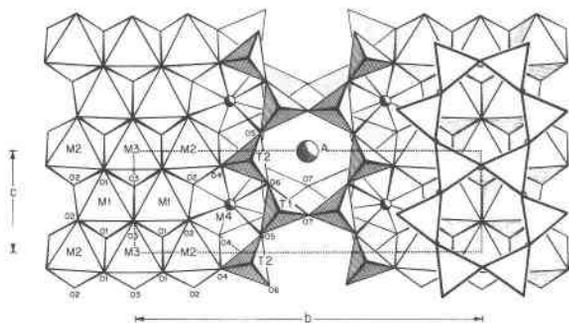
Fig. 1. Projection of the *I2/m* richterite structure onto the (100) plane.

both richterites in the *I2/m* and *C2/m* space groups are given in Table A10.

We use the MTEC (mean thermal expansion coefficient) of Cameron et al. (1973a) to describe variations in the unit cell parameters and interatomic distances with increasing temperature. MTEC is defined as $\alpha_x = 1/X_{24} \cdot (X_T-X_{24}/T-24)$, where X_{24} is the value of a parameter at room temperature and $(X_T-X_{24}/T-24)$ is the slope obtained from least squares analysis.

Room temperature richterite structures

A projection of the monoclinic *I2/m* amphibole structure onto the (100) plane is shown in Figure 1. Although the general structure has been described in numerous publications (*e.g.*, Papike *et al.*, 1969; Cameron and Papike, 1979), salient features to note include the following. The double tetrahedral chains that lie parallel to *c* contain two types of tetrahedra. T1 is coordinated by three bridging and one non-bridging (O1) oxygen atom, and T2 is coordinated by two bridging and two non-bridging (O2,O4) oxygen atoms. The degree of kinking of the tetrahedral chains is given by the O5–O6–O5 tetrahedral chain angle. Variations in the chain angle affect the ditrigonality of the 6-membered tetrahedral rings. There are four types of M polyhedra which form wide bands that also extend parallel to *c*. The cations occupying M1, M2, and M3 are octahedrally coordinated whereas that in M4 is 8-coordinated. The M1 cation is coordinated by four oxygen and two (OH,F) atoms in a *cis* arrangement. M3 is coordinated by four oxygen and two (OH,F) atoms that are in a *trans* arrangement. M2 is coordinated by six oxygen atoms and M4 by eight oxygen atoms. The A site, which is located between the backs of adjacent tetrahedral chains, is in a large cavity formed by 12 oxygen atoms (four O7's, four O6's, and four O5's) that lie within approximately 4.0Å. The site is variously described as 8–12-coordinated by different researchers.

The richterites examined in this paper have identical chemistry except for the A cation. In K richterite the A site is completely filled by K, and in Na richterite it is completely occupied by Na. In both amphiboles, the M1, M2, and M3 sites contain Mg and the M4 site a 1:1 ratio of

Ca and Na. Both contain only fluorine in the O3 position. As expected, the structures of the two richterites are similar because of the similarity in their chemistry. The mean T–O bond lengths in both structures are statistically identical, with the T1 tetrahedra being significantly smaller and less distorted than the T2 tetrahedra (Table A3). Mean bond lengths for comparable M octahedra in both richterites are also similar (Table A5). The M2 octahedron, which has six oxygen ligands, is the largest (mean M2–O ≃ 2.087Å) and least distorted of the three octahedra. The M1 and M3 octahedra, which have two fluorine and four oxygen ligands, have significantly different mean M–O values (mean M1–O ≃ 2.051Å *vs.* mean M3–O ≃ 2.043Å in each richterite). Cameron and Gibbs (1973) observed essentially identical mean M1–O and M3–O distances in a synthetic fluor-tremolite. The mean M4–O distance is significantly different in the two structures (2.555Å for K richterite *vs.* 2.544Å for the Na richterite) even though the sites have identical occupancies. The difference may result from the presence of the larger K atom in the adjacent A site in K richterite. In fact, careful examination of the small differences in the mean M–O distances in Table A5 reveals a systematic trend—*i.e.*, the mean bond lengths for octahedra in the K richterite are always slightly larger than those for the Na richterite. A similar effect is observed in the M2 site of pyroxenes (*e.g.*, Clark *et al.*, 1969; Ribbe and Prunier, 1977). For identical M2 occupancy in end-member Ca, Na, and Li pyroxenes, the mean M2–O distance increases as the size of the cation in the adjacent M1 site increases.

The split-atom models adopted for the A sites in the two richterites are shown in Figure 2. In the ½ atom approximation used for K richterite, K occupies randomly two symmetrically-equivalent atom sites (special position 4*i*) that lie within the (010) mirror plane. The atom sites have slightly different heights in the *a** direction, and the vector between them has a length of ~0.29Å and is oriented roughly parallel to the elongate cavity formed by the two slightly displaced tetrahedral rings (Fig. 3a). In the ¼ atom approximation adopted for the Na richterite, the Na atom has an equal probability of occupying one of four general positions (8*j*) (Fig. 3b). At room temperature, the distance between sites across the mirror is ~0.47Å whereas that across the twofold axis is ~0.53Å.

ΔF maps calculated with the A atom removed are shown in Figure 4. Contour intervals are indicated on each figure, but the maps are not on an absolute scale. Parts of the maps produced by the twofold axes and the mirror planes are omitted. The figures on the left show the (*ac*) plane, and those on the right the (*bc*) plane; the upper row is at 24°C and lower row at 800°C. At room temperature single elongate peaks are present in the (*ac*) plane of both structures. In the 24°C data for the (*bc*) plane the electron density in the proximity of the A site extends much farther along the *b* axis in Na richterite than in K richterite. Because Na has half as many electrons as K, this distribution supports our assumption
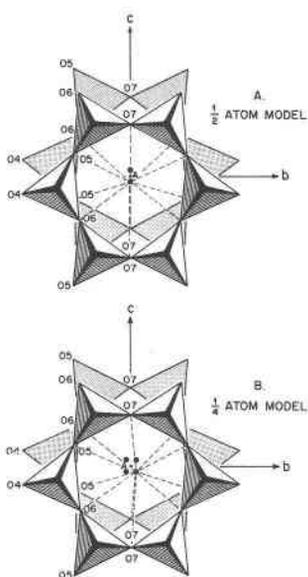
Fig. 2. Split-atom models adopted for the A cations in richterites. Small dot at the intersection of the (010) mirror and the twofold axis parallel to b represents the ideal ordered position of the A cation. A. Half-atom model of K richterite. The single K atom is replaced by two half atoms constrained to the (010) mirror plane (special position 4i). B. Quarter-atom model of Na richterite. The single Na atom is replaced by four quarter atoms at the general position 8j.

Fig. 3. A-site coordination as viewed down the b axis. Only one of the split A atoms is included. X's mark the location of the split A atoms not shown. Total number of oxygen atoms is twelve. Each O5 and O6 atom represents two atoms that are superimposed in this projection. Axes for both the I and C-centered cells are shown. Ellipsoids are drawn at 75% probability using the ORTEP program of Johnson (1965). A. 24°C K richterite. B. 24°C Na richterite. The positions of two additional quarter atoms are not visible because they lie directly beneath the two A atoms shown.

that the Na atom is displaced from the mirror plane. In addition, examination of these ac and bc maps and parallel sections in Na richterite show that in three-dimensions the electron density distribution has a disc-like shape with no distinct nodes.

The oxygen coordination of the K atom at special position 4i and the Na atom at general position 8j involves eight short (<3.01Å) and three long (<3.55Å) bonds. The mean interatomic A–O distance for an 8-coordinated Na atom is 2.78Å and for an 8-coordinated K atom is 2.85Å (Table A7). This compares with mean ^{VIII}Na–O values of ~2.74Å in albite (Winter *et al.*, 1979) and ~2.62Å in nepheline (Foreman and Peacor, 1970), and mean ^{VIII}K–O values of ~2.93Å for microcline (Finney and Bailey, 1964). The Na and K atoms in mica structures typically have only six coordinating oxygens within ~3.1Å.

Structural variations with increasing temperature

Unit cell parameters

The variation with increasing temperature of unit cell parameters is approximately linear for both richterites (Fig. 5). Mean thermal expansion coefficients (MTEC) for the c direction are an order of magnitude smaller than those for the a or b directions. In addition, expansion in the a and b directions is significantly greater in the K richterite than in the Na richterite (Table 3). The β_I angle

Fig. 4. ΔF maps calculated with the A atoms removed. The maps are not on an absolute scale, and portions produced by the twofold axes and mirror planes are omitted. The (ac) plane is shown on the left and the (bc) plane on the right. The upper row is for 24°C data and the lower row for 800°C data.
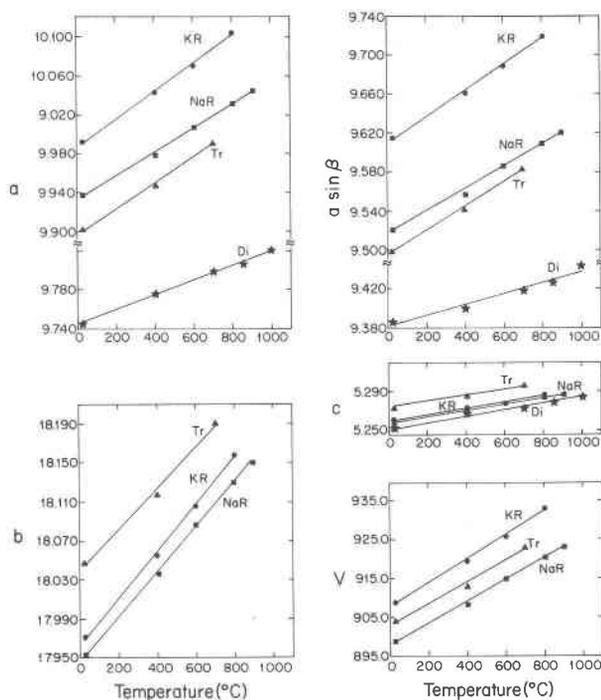
Fig. 5. Variation with increasing temperature of unit cell parameters of richterites, tremolite, and diopside (after Cameron and Papike, 1979). KR = K richterite, NaR = Na richterite, Tr = tremolite, and Di = diopside. I-centered cell parameters of the amphiboles are plotted.

in K richterite remains approximately constant over the temperature interval studied. The β_I angle in Na richterite increases slightly between 24° and 400°C, and then does not change (within 2 e.s.d.) up to 900°C. The relative magnitudes of the MTEC's for the cell parameters must be interpreted with caution because the crystallographic axes do not necessarily coincide with the axes of the thermal expansion ellipsoid. The only constraint which symmetry imposes in a monoclinic crystal is that one axis of the thermal ellipsoid must coincide with the b crystallographic axis. The other two ellipsoid axes thus lie in the (010) plane, but not necessarily coincident with the a or c crystallographic axes.

Polyhedral expansions

With increasing temperature both richterite structures exhibit differential polyhedral expansion, i.e., the various types of coordination polyhedra expand at different rates. This phenomenon, which is well documented in other studies (e.g., Cameron et al., 1973a; Lager and Meagher, 1978), is related to charge, coordination number, and electronegativity of the cation involved. In the richterites described here, MTEC's increase in the following order: T1 = T2 ≪ M1 ≃ M2 ≃ M3 < M4 < ^{X}A. Similar variations were observed in tremolite (Sueno et al., 1973) and cummingtonite (Sueno et al., 1972).

Mean Si–O bond lengths of the T1 and T2 tetrahedra in both richterites remain approximately constant with in-

Table 3. Mean thermal expansion coefficients ($°C-1 \times 10^5$) in richterites

	K fluor-richterite (24°-800°C)	Na fluor-richterite (24°-900°C)	Tremolite[a] (24°-700°C)	Diopside[b] (24°-1000°C)
Cell Parameters[c]				
a_I	1.43	1.23	1.36	--
b_I	1.34	1.27	1.17	--
c_I	0.61	0.62	0.58	--
V_I	3.39	3.10	3.13	--
a_C	1.27	1.08	1.20	0.78 [d]
b_C	--	--	--	2.05
c_C	--	--	--	0.65
V_C	--	--	--	3.33
Mean Interatomic Distances				
M1	1.35	1.16	1.35	1.44
M2	1.56	1.25	1.63	--
M3	1.30	1.33	1.15	--
^{VIII}M4(M2)[d]	1.76	1.56	1.65	1.64
^{VIII}A	0.83	1.14	--	--
^{X}A	2.38	2.15	1.30	--
^{XI}A	1.64	1.50	--	--
Volumes of Polyhedra				
M1	--	3.54	4.31	4.26
M2	4.25	3.50	4.86	--
M3	--	3.91	3.62	--
^{VIII}M4(M2)[e]	--	4.34	4.5	4.42

[a] Sueno et al. (1973)
[b] Cameron et al. (1973)
[c] Subscript I indicates I2/m space group and C indicates C2/m space group.
[d] C-cell of tremolite is analogous to I-cell of richterites and tremolite.
[e] Site labels in parentheses refer to diopside.

creasing temperature (Fig. 6; Table A3). The mean values at all temperatures are within two standard deviations of those at room temperature. Distortion of the tetrahedra, as quantified by the quadratic elongation parameter of Robinson *et al.* (1971), also remains approximately constant. Variations in individual T–O interatomic distances are usually within three standard deviations of the room temperature values. The O–O distances and O–T–O angles also show small, but non-systematic variations with increasing temperature (Tables A3 and A4). A similar lack of variation was observed in tremolite (Sueno *et al.*, 1973) and clinopyroxenes (Cameron *et al.*, 1973a). The O5–O6–O5 tetrahedral chain in both richterites straightens (*i.e.*, moves toward 180°) with increasing temperature. In K richterite it increases 2.8° over ~800°C, and in Na richterite it increases 3.6° over 900°C.

Mean interatomic distances in the M polyhedra increase significantly with increasing temperature (Fig. 6, Table A5). In both richterites, the 8-coordinated M4 site has a higher MTEC than the octahedrally-coordinated M1, M2, and M3 sites. Mean bond lengths for the latter sites expand in the sequence M2 > M1 > M3 in K richterite and M3 > M2 > M1 in Na richterite. The M3 octahedron, which lies near the center of the octahedral strip, has similar MTEC's in both richterites (Table 3). The M1 and M2 octahedra, which lie on the edge of the octahedral strip, have significantly higher MTEC's in the K richterite than in the Na richterite. The higher values may be a result of the higher rates of expansion of the large K atom in the A site of the K richterite. With increasing temperature, M2 is the only one of the three regular octahedra to exhibit a significant increase in distortion (Table A5). The magnitudes of the MTEC values for K richterite are very similar to those of tremolite (Sueno *et al.*, 1973).

The behavior of individual bonds within each of the M polyhedra is largely dependent on their orientation in the structure. In the M1 and M3 octahedra the bonds that lie in or close to the (010) plane (*e.g.*, M1–O1 and M3–O3) typically expand less than the bonds that lie parallel to the *b* axis. In the M2 octahedron, the rate of expansion of the M2–O2 bond is comparable to M2–O4 and both rates are significantly smaller than that of the M2–O1 bond. The bonds involving fluorine atoms have rates of expansion that are comparable to those involving oxygen. In the M3 octahedron, where fluorine is in a *trans* arrangement in the (010) plane, its rate of expansion is significantly less than that of the Mg–O bonds. However, in the M1 octahedron, fluorine is in a *cis* arrangement and the reverse is true.

The expansion of individual bonds in the 8-coordinated M4 site is affected both by their orientation and by the type of oxygen involved. The O2 and O4 oxygens, which are shared with other M sites, and the O5 and O6 oxygens, which are shared with the tetrahedral chains, behave differently. The bonds to the non-bridging O2 and O4 oxygen atoms show rates of increase that are comparable to those of the regular 6-coordinated M polyhedra.
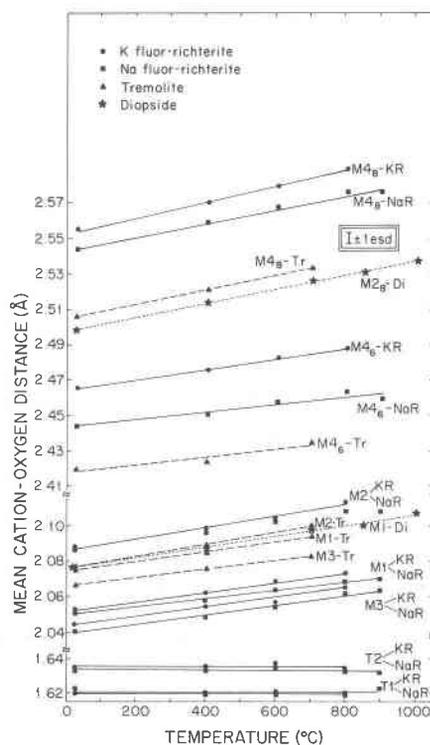
Fig. 6. Variation with increasing temperature of mean cation-oxygen distances in richterites (KR = K richterite, NaR = Na richterite), tremolite (Tr), and diopside (Di). The subscript number indicates the number of ligands used in calculating the mean bond length.

As in the M1 and M3 octahedra, the bonds lying approximately in the (010) plane have small MTEC's. Bonds involving the bridging oxygen atoms O5 and O6, which are affected by straightening of the tetrahedral chains and their relative displacement, have the most atypical MTEC's. The M4–O5 distance exhibits a significantly higher MTEC than any other individual M–O bond in the four M polyhedra whereas the M4–O6 distance remains approximately constant (K richterite) or decreases slightly (Na richterite).

MTEC's for 10-coordinated mean A–O distances are significantly larger than those of the M sites (Table 3), but MTEC's for 11-coordinated mean A–O distances are comparable to those of the M sites. Variations in mean and individual bond distances for both richterites are shown in Figures 6 and 7. The mean of the A site atoms plotted in Figure 6 is the average of the shortest eight A–O bonds shown in Figure 7. The three longest bonds (two O6's and one O7) show high rates of change with increasing temperature because they are affected significantly by straightening of the tetrahedral chains and movement of the chains relative to each other. For example, the high rate of increase of the A–O6 distances is a result of straightening of the O5–O6–O5 chain angle, which moves the O6 oxygen atoms away from the A atom. The decrease in the A–O7 distances is caused by increased
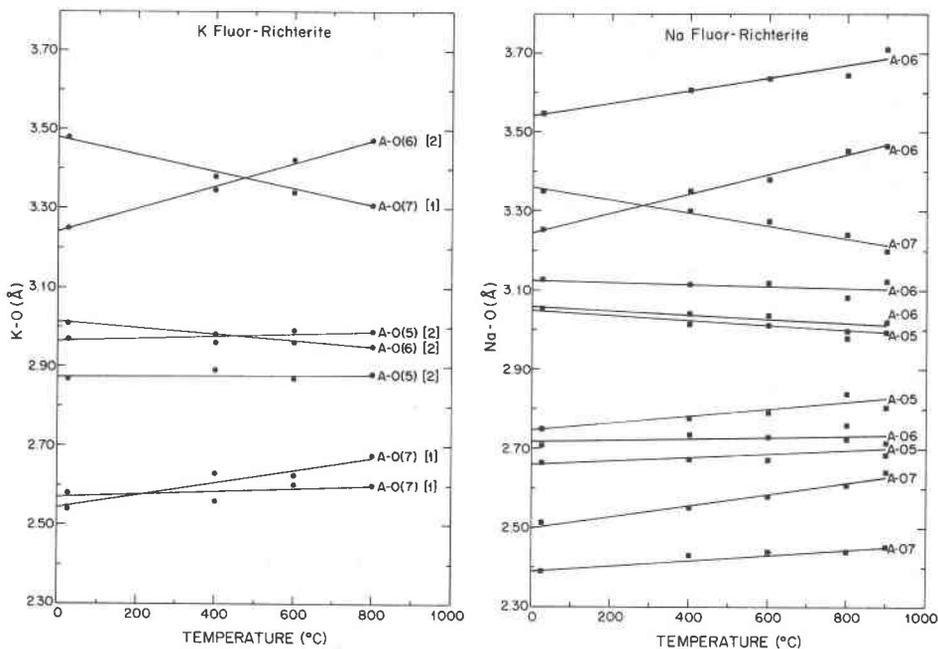
Fig. 7. Variation with increasing temperature of individual A–O bonds. A. K richterite. Numbers in brackets are bond multiplicities. B. Na richterite. All bonds have a multiplicity of one.

displacement of the tetrahedral chains relative to each other. In Figure 8 the rates of increase of mean A–O distances in the richterites are compared to that of a mean A–O distance for a hypothetical A atom in tremolite.

In K richterite the distance between the split-atom

Fig. 8. Variation with increasing temperature of mean A–O bonds in richterites and tremolite. Symbols are the same as in Fig. 6.

positions increases from ~0.29Å at room temperature to ~0.53Å at 800°C. In Na richterite, the distance between the two atom sites on either side of the mirror decreases from 0.47Å to 0.41Å whereas the distance between the two sites on opposite sides of the twofold axis increases from ~0.53Å to ~0.73Å. The ΔF maps (Fig. 4) of the A site in both structures show that the shape of the electron density distribution at 800°C is similar to that at room temperature.

Thermal parameters

Equivalent isotropic temperature factors of both the cations and anions in the Na and K richterite increase regularly over the temperature ranges investigated (Table A2; Fig. 9). The rate of increase in $B(Å^2)$ of cations increases from 4-coordinated Si to 6-coordinated Mg to 8-coordinated (NaCa) in the M4 site. The rates are almost identical for cations occupying equivalent sites in the two structures, and in addition, the variation among atoms in similar sites (*e.g.*, M1, M2, M3) within the same structure is small. For this reason, we have not plotted individual curves for the atoms in the M1, M2, M3 and T1,T2 sites in Figure 9. The stippled field labelled Si(T1,T2) contains four curves whereas the field labelled Mg(M1,M2,M3) contains six curves. Also plotted are $B(Å)^2$ for Si, Mg, and Ca in tremolite and diopside.

The curves for the anion temperature factors of both richterites lie just above the stippled field of the Mg atoms. Their rates of increase with increasing temperature are also roughly correlated with coordination num-

ber. The O3 and O4 atoms, which have the lowest coordination number (three), exhibit the highest rates of increase. The apical O1 and O2 atoms, which are surrounded by four close cations, exhibit the lowest rates of increase. The remaining anions, O5, O6, O7, have rates of increase that are intermediate between these two extremes. These three oxygen atoms are 4-coordinated but, in addition, all are bonded to the A cation. The A–O bonds are long, presumably weaker, and thus they do not physically constrain the movement of the anion as much as closer atoms might. The temperature factor of the fluorine atom in the O3 site is higher than OH in tremolite (Sueno et al., 1973) at room temperature, and its rate of increase with increasing temperature is also larger. With the exception of O3, the rates of increase of the anion $B(Å^2)$ are lower in the richterites than in tremolite.

The only M cation with a highly anisotropic thermal ellipsoid is the (NaCa) atom in M4 (Figs. 10 and 11; Tables A8 and A9). This site lies on a twofold axis parallel to b, and thus one of the thermal ellipsoid axes coincides with b and the other two lie in the (010) mirror plane. In both richterites at all temperatures the M4 thermal ellipsoid is prolate with its longest axis in the (010) plane, approximately perpendicular to the O4–M4–O4 direction (Fig. 11). The prolate shape is consistent with essentially pure thermal vibration and indicates little positional disorder at the site even though it is occupied by two types of cations. Positional disorder involving M4 cations with different ionic radii is usually manifested in an oblate thermal ellipsoid whose shortest axis is perpendicular to b. The electron density is smeared out along the b axis because the different-sized cations occupy slightly different positions along the axis. Ca and Na have similar ionic radii, and thus they probably occupy similar positions along the b axis. Comparable ellipsoid orientations and shapes were noted for the Ca atom in M4 in tremolite (Sueno et al., 1973) and in M2 in diopside (Cameron et al., 1973a).

The thermal ellipsoid of the split A atom in both structures is prolate, with that of the Na atom in Na richterite being more anisotropic. The ellipsoid associated with the K atom in K richterite, which was refined as a ½ atom in the (010) plane, has an orientation similar to that of the M4 cation (Fig. 3). The longest ellipsoid axis lies within the (010) plane midway between $-a_I$ and c_I. In the Na richterite the longest ellipsoid axis also lies in the (010) plane and midway between $-a_I$ and c_I. The intermediate ellipsoid axis, which is parallel to b in the K richterite, lies in the (010) plane at ~70° to the b axis.

Among the anions, ellipsoids for O1 and O2 are the least anisotropic at all temperatures examined. The O3 ellipsoid ($\equiv$ fluorine) in Na richterite is prolate at all temperatures except 900°C whereas in K richterite it varies in shape from prolate to oblate (Fig. 10). The O4, O5, O6, and O7 ellipsoids are moderately anisotropic at all temperatures studied, with the anisotropy of O4 and O7 being most pronounced.
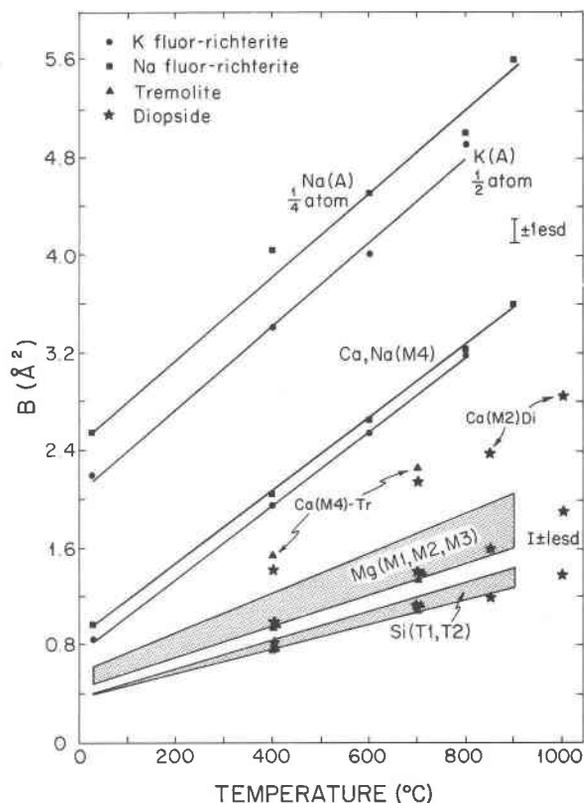
Fig. 9. Variation with increasing temperature of equivalent isotropic temperature factors of cations in richterites, tremolite, and diopside. Data for tremolite and diopside are shown as triangles and stars, respectively, with no best fit line. The stippled field labelled Si(T1,T2) shows the range in variation for four richterite curves. The field labelled Mg(M1, M2, M3) represents the variation for six richterite curves.

Discussion

Room temperature structures

The structure of the synthetic K richterite examined in this study is generally similar to the natural K richterite studied by Papike et al. (1969). Mean T1–O and mean T2–O distances and the O5–O6–O5 tetrahedral chain angle are slightly larger in the natural richerite, but the absolute values in both richterites are identical within three standard deviations. The mean octahedral M distances in the natural richterite are significantly larger, and reflect the substitution of small amounts of Fe^{2+} and Mn for Mg in the octahedral sites and OH for fluorine in the O3 site. These substitutions increase the mean M–O distances because the atomic species being introduced have larger effective ionic radii than those being replaced. In addition, it appears likely that the O3 site in the natural richterite contains an appreciable amount of fluorine because the mean M–O bond distances are not as large as expected for a pure OH-richterite. Substitution of OH for F in tremolite (Cameron and Gibbs, 1973) causes an
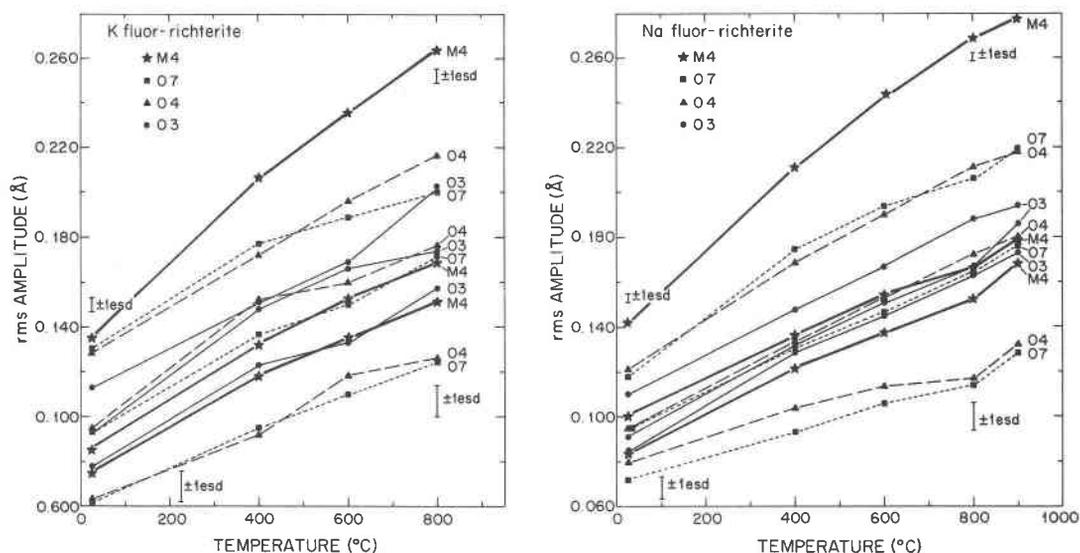
Fig. 10. Variation of the magnitude of the three principal axes of the thermal ellipsoids for the M4, O3, O4, and O7 atoms. A. K richterite. B. Na richterite.

increase of ~0.02Å in the mean M1 and M3 distances. The difference observed between the two K richterites is only ~0.01Å, and this includes the increase caused by the substitution of larger cations in these sites.

Positional disorder of A cations

Positional disorder of cations in the A site of amphiboles was first recognized in 1968 by Gibbs and Prewitt, and since that time, most refinements of amphibole structures have been done with the A cations disordered. The types of disorder proposed by various authors involve displacements within the mirror plane at special position 4i (*e.g.*, Gibbs and Prewitt, 1968; Papike *et al.*, 1969), along the twofold axis at special position 4g (*e.g.*, Gibbs and Prewitt, 1968; Hawthorne and Grundy, 1972, 1973a,b), and at the general position 8j (Cameron *et al.*, 1973b,c). The principal factors that seem to influence the direction of the disorder include: (1) the cation species (K *vs.* Na) present at the A site, (2) the anion species (OH *vs.* F *vs.* O^{2-}) present at the O3 site, and (3) the distribution of tetrahedral Al. Hawthorne and Grundy (1978) and Docka *et al.* (1980) recently discussed these factors. The latter authors calculated electrostatic structure energies in order to model possible causes for the disorder. Their results indicate that factors noted in (2) and (3) control, to a large extent, the positional disorder of the A cation. Hawthorne and Grundy, though recognizing the importance of tetrahedral Al, concluded that the character of the disorder is largely a function of cation type. In their ideal model, K disorders at the special position 4i and Na at the special position 4g. Both sets of authors indicate that occupancy of the M sites also affects the disordering, but to a lesser degree.

The reason for the positional disordering of the A cations in the synthetic richterites of this study is less

obvious. The effect of Al is precluded because, unlike the natural amphiboles, these richterites contain no tetrahedral Al. Factors that may be important are bond strength requirements about the A and M4 cations. A coupled relationship, similar to that which may exist between tetrahedral Al and disordered A cations, may also exist between (Ca,Na) in the M4 site and the disordered A cations. Such an association would also explain the direction of Na disordering—off the special position 2b directly toward the M4 sites. Bond strength sums to the K atom in the synthetic richterite are similar to those of natural amphiboles with K in their A sites (Hawthorne and Grundy, 1978). The bond strength at room temperature for an 11-coordinated K atom is 1.265 v.u. and for an 8-coordinated atom is 1.07 v.u. (Table 4). The synthetic Na richterite, however, behaves differently than natural amphiboles with Na in the A site. The deficiency in bond strength sums observed for natural amphiboles (~0.88–0.92 v.u.; Hawthorne and Grundy, 1978) is not present in the synthetic Na richterite. The sum for an 11-coordinated site is 1.002 v.u. at room temperature. (The difference in behavior of the synthetic richterites could be related, in part, to the absence of tetrahedral Al.) Bond strength sums for the Na and K cations in the ideal position at the intersection of the mirror and twofold axis are also given in Table 4. The values are very similar to those for the room temperature disordered models, and thus bond strength requirements about the A cation *alone* do not seem to be a significant driving force in the disordering.

High temperature structures

With increasing temperature the major changes that take place in the richterite structure include: first, an increase in the size of all cation polyhedra with the exception of the silica tetrahedra; second, a 3–4° increase

Fig. 11. M4 coordination as viewed down the *b* axis. Axes for both the I and C-centered cells are shown. Ellipsoids are drawn at 75% probability using the ORTEP program of Johnson (1965). Diagrams are drawn for 24°C data. A. K richterite. Dashed ellipsoid drawn for M4 cation at 800°C. B. Na richterite. Dashed ellipsoid drawn for M4 cation at 900°C.

Table 4. Strengths (v.u.)[a] of A–O bonds in richterites

	24°C	24°C	400°C	600°C	800°C	900°C
K fluor-richterite	A = 2b (2/m)	A = 4i (m)	A = 4i (m)	A = 4i (m)	A = 4i (m)	--
A-O5	0.115 [4][b]	0.123 [2]	0.119	0.123	0.121	--
A-O5	--	0.106 [2]	0.107	0.103	0.103	--
A-O6	0.084 [4]	0.100 [2]	0.104	0.107	0.109	--
A-O6	--	0.071 [2]	0.062	0.056	0.053	--
A-O7	0.207 [2]	0.213 [1]	0.182	0.182	0.168	--
A-O7	--	0.199 [1]	0.206	0.192	0.192	--
A-O7	0.044 [2]	0.053 [1]	0.059	0.062	0.065	--
Σ (8 bonds)	--	1.070	1.048	1.040	1.026	--
Σ (10 bonds)[c]	1.210	1.212	1.172	1.152	1.132	--
Σ (11 bonds)	--	1.265	1.231	1.214	1.197	--
Σ (12 bonds)	1.298	--	--	--	--	--
Na fluor-richterite	A = 2b (2/m)	A = 8j	A = 8j	A = 8j	A = 8j	A = 8j
A-O5	0.086 [4]	0.120 [1]	0.118	0.118	0.109	0.114
A-O5	--	0.104 [1]	0.098	0.098	0.090	0.095
A-O5	--	0.067 [1]	0.071	0.071	0.074	0.070
A-O5	--	0.060 [1]	0.060	0.060	0.064	0.060
A-O6	0.060 [4]	0.111 [1]	0.106	0.107	0.102	0.111
A-O6	--	0.066 [1]	0.068	0.068	0.072	0.070
A-O6	--	0.050 [1]	0.045	0.043	0.039	0.038
A-O6	--	0.035 [1]	0.032	0.031	0.031	0.029
A-O7	0.181 [2]	0.190 [1]	0.177	0.174	0.174	0.170
A-O7	--	0.154 [1]	0.144	0.137	0.130	0.124
A-O7	0.030 [2]	0.045 [1]	0.048	0.049	0.051	0.054
Σ (8 bonds)	--	0.872	0.842	0.833	0.815	0.814
Σ (10 bonds)	0.946	0.957	0.919	0.907	0.885	0.881
Σ (11 bonds)	--	1.002	0.967	0.956	0.936	0.935
Σ (12 bonds)	1.006	--	--	--	--	--

[a] Bond strengths calculated using the universal curves of Brown and Shannon (1973).
[b] Numbers in brackets are bond multiplicities.
[c] Includes four A-O5, four A-O6, and two A-O7 bonds.

Straightening of the chains, in turn, decreases the ditrigonal character of the tetrahedral rings, increases the M4–O5 interatomic distances, and causes the M4 site to become more 6-coordinated. Straightening of the tetrahedral chains is also correlated with increasing displace-

Table 5. Coordination coefficients and tetrahedral chain displacements in richterites and tremolite

	Coordination Coefficient of M4[a]	Tetrahedral Chain Displacement Factor[b]
K fluor-richterite		
24°C	1.037	0.1856
400°C	1.038	0.1872
600°C	1.039	0.1884
800°C	1.041	0.1891
Na fluor-richterite		
24°C	1.041	0.2125
400°C	1.044	0.2150
600°C	1.045	0.2140
800°C	1.046	0.2147
900°C	1.048	0.2151
Tremolite		
24°C	1.036	0.1985
400°C	1.040	0.2015
700°C	1.041	0.2034

[a] Coordination coefficient = (8-coordinated mean M4-O/6-coordinated mean M4-O).
[b] Tetrahedral chain displacement d is the distance between the centers of two opposing six-membered tetrahedral rings. See Sueno et al. (1973) for a more detailed explanation.

in the silicate chain angle, O5–O6–O5, with an attendant decrease in ditrigonal character of the tetrahedral rings; and third, increased displacement of the tetrahedral chains above and below the A site. The various polyhedra expand differentially, but in a sequence (T ≪ ^{VI}M < ^{VIII}M) recognized in other silicate minerals. The relative rate of expansion can be generally related to the strength of the bonds to individual cations. Smaller values of the MTEC for mean bond lengths are associated with lower coordination number and higher charge on the cations.

The differential polyhedral expansion produces a potential misfit between the octahedral and tetrahedral layers. Maintaining the linkage between the relatively inert tetrahedra and the expanding M sites with increasing temperature induces secondary changes such as the extension or straightening of the silicate chains. In K richterite the O5–O6–O5 angle increases ~2.8° over 800°C, and in Na richterite it increases 3.6° over 900°C.

ment of tetrahedral chains in adjacent layers if a constant O4–O4 distance is assumed. The tetrahedral chain displacements, calculated using the method of Sueno et al. (1973), are given in Table 5.

The behavior of the richterite structures with increasing temperature is generally similar to that observed in tremolite (Sueno et al., 1973). The only chemical differences between the richterites and tremolite involve occupancy of the M4 site (Ca in tremolite and Ca+ Na in richterite) and the A site (vacant in tremolite and filled with K or Na in the richterites). Thus, it is not unexpected that the tetrahedral and regular octahedral (M1, M2, M3) sites in the structure exhibit similar variations with increasing temperature. MTEC's for the mean M4–O distances in tremolite are also comparable to those in richterite even though occupancies of the site are different in the structures. Expansion around the A site is significantly less in tremolite than in either of the richterites (Fig. 8). MTEC's of mean Mg-O bond lengths observed for diopside ($\sim$1.15–1.65/°C $\times$ 10^{-5}; Table 3) are comparable to those of the richterites and tremolite; however, MTEC's for the mean octahedral Mg–O bonds in forsterite (Smyth and Hazen, 1973; Hazen, 1976) are 1.24/°C $\times$ 10^{-5} for M1 and 2.44/°C $\times$ 10^{-5} for M2. The atypically large expansion of the M2 polyhedron in forsterite may be related in part to the number of edges that it shares with adjacent polyhedra. It shares only three edges in contrast to the M1 octahedron in forsterite and the Mg octahedra in the richterites, tremolite, and diopside, all of which share five or six edges. The increased edge-sharing apparently has a greater constraining effect on the thermal expansion of the polyhedra, and results in different behavior with increasing temperature. These comparisons indicate that it may be reasonable to extrapolate thermal expansion data between structurally similar groups such as amphiboles and pyroxenes, but not between groups as different as amphiboles and olivines.

The MTEC of the K richterite unit cell volume is slightly larger than that for Na richterite (3.39 vs. 3.10/°C $\times$ 10^{-5}). The value for Na richterite is essentially identical to tremolite (3.13/°C $\times$ 10^{-5}), even though the MTEC's of polyhedra in tremolite are more similar to those of K richterite. The lower value of the MTEC of the tremolite unit cell volume is apparently a result of the lower rate of expansion of its A site cavity relative to that of the richterites. The MTEC of 10-coordinate mean A-O distances in both richterites is significantly greater than that in tremolite (2.38 and 2.15 vs. 1.30/°C $\times$ 10^{-5}).

Conclusions

1. With increasing temperature, the mean T1–O and T2–O interatomic distances in both K and Na richterites remain statistically identical to room temperature values.

2. Thermal expansion of the octahedrally-coordinated M1, M2, and M3 sites is much greater than that of the tetrahedral sites, but less than that of the 8-coordinated M4 site. Relative MTEC's for mean polyhedral distances

in the K richterite are M3 < M1 < M2 and in the Na richterite, M1 < M2 < M3. The thermal expansion coefficients are generally similar to those of analogous octahedra in tremolite and diopside.

3. The MTEC's of the mean interatomic distances for the M4 sites in both richterites are generally comparable to those of tremolite and diopside even though the site occupancies are different [M4 = (Ca,Na) in richterites; M4 = Ca in tremolite and diopside].

4. Thermal expansion of the A polyhedron in K richterite is slightly greater than that of the A polyhedron in Na richterite. Expansion in both richterites is significantly larger than that in tremolite, where the A site is vacant.

5. The A atoms of both richterites were approximated by split-atom models at all temperatures. The K atom in K richterite was refined with a ½ atom model in which K was confined to the special position $4i$ within the (010) mirror plane. The Na atom in the A site of Na richterite was refined using a ¼ atom model with the Na on a general position $8j$ that lies off both the (010) mirror plane and the twofold axis parallel to b.

6. Unit cell parameters of the richterites vary linearly as a function of temperature, with MTEC's in K richterite increasing as $c < b < a$ and in Na richterite as $c < a < b$. The β angle in both richterites varies less than one degree over the temperature intervals studied.

7. The rate of increase of equivalent isotropic temperature factors of the cations can be related to coordination number. The 4-coordinated Si atoms have the lowest rate of increase whereas the 8–11 coordinated cations in the A sites have the highest rate of increase. The rate of increase of the (Na,Ca) atoms in the richterites is greater than that of the Ca atoms in tremolite.

8. The thermal ellipsoid for the M4 atom is highly anisotropic. In both structures at all temperatures, it is prolate with the longest axis in the (010) plane and approximately perpendicular to the O4–M4–O4 direction. The shape of the ellipsoid indicates little positional disorder along the b axis.

9. Among the anions, the thermal ellipsoids of O4 and O7 are the most anisotropic and those for O1 and O2 are the least anisotropic at elevated temperatures.

References

Brown, G. E. and Prewitt, C. T. (1973) High temperature crystal chemistry of hortonolite. American Mineralogist, 58, 577–587.

Brown, G. E., Sueno, S., and Prewitt, C. T. (1973) A new single-crystal heater for the precession camera and four-circle diffractometer. American Mineralogist, 58, 698–704.

Brown, I. D. and Shannon, R. D. (1973) Empirical bond-strength–bond-length curves for oxides. Acta Crystallographica, A29, 266–282.

Cameron, M. and Gibbs, G. V. (1973) The crystal structure and bonding of fluor-tremolite: a comparison with hydroxyl tremolite. American Mineralogist, 58, 879–888.

Cameron, M. and Papike, J. J. (1979) Amphibole crystal chemistry: a review. Fortschritte der Mineralogie, 57, 28–67.

Cameron, M., Sueno, S., Prewitt, C. T., and Papike, J. J. (1973a) High-temperature crystal chemistry of acmite, diopside, hedenbergite, jadeite, spodumene and ureyite. American Mineralogist, 58, 594–618.

Cameron, M., Sueno, S., Prewitt, C. T., and Papike, J. J. (1973b) High temperature crystal chemistry of K-fluor-richterite. (abstr.) American Geophysical Union Transactions, 54, 497–498.

Cameron, M., Sueno, S., Prewitt, C. T., and Papike, J. J. (1973c) High temperature crystal chemistry of Na-fluor-richterite. (abstr.) American Geophysical Union Transactions, 54, 1230.

Clark, J. R., Appleman, D. E., and Papike, J. J. (1969) Crystal-chemical characterization of clinopyroxenes based on eight new structure refinements. Mineralogical Society of America Special Paper, 2, 31–50.

Docka, J. A., Bish, D. L., and Burnham, C. W. (1980) Positional disorder in clinoamphibole "A" sites. (abstr.) Geological Society of America Abstracts with Programs, 12, 414.

Doyle, P. A. and Turner, P. A. (1968) Relativistic Hartree–Fock X-ray and electron scattering factors. Acta Crystallographia, A24, 390–397.

Finney, J. J. and Bailey, S. W. (1964) Crystal structure of an authigenic maximum microcline. Zeitschrift für Kristallographie, 119, 413–436.

Foreman, N. and Peacor, D. R. (1970) Refinement of the nepheline structure at several temperatures. Zeitschrift für Kristallographie, 132, 45–70.

Gibbs, G. V. and Prewitt, C. T. (1968) Amphibole cation site disorder. (abstr.) In International Mineralogical Association, Papers and Proceedings of the Fifth General Meeting, p. 334–335. Mineralogical Society, London.

Hawthorne, F. C. and Grundy, H. D. (1972) Positional disorder in the A site of clinoamphiboles. Nature, 235, 72–73.

Hawthorne, F. C. and Grundy, H. D. (1973a) The crystal chemistry of the amphiboles. I. Refinement of the crystal structure of ferrotschermakite. Mineralogical Magazine, 39, 36–48.

Hawthorne, F. C. and Grundy, H. D. (1973b) The crystal chemistry of the amphiboles. II. Refinement of the crystal structure of oxy-kaersutite. Mineralogical Magazine, 39, 390–400.

Hawthorne, G. F. and Grundy, H. D. (1978) The crystal chemistry of the amphiboles. VII. The crystal structure and site chemistry of potassian ferri-taramite. Canadian Mineralogist, 16, 53–62.

Hazen, R. M. (1976) Effects of temperature and pressure on the crystal structure of forsterite. American Mineralogist, 61, 1280–1293.

Huebner, J. S. and Papike, J. J. (1970) Synthesis and crystal chemistry of sodium-potassium richterites (Na,K)NaCaMg$_5$Si$_8$O$_{22}$(OH,F)$_2$: a model for amphiboles. American Mineralogist, 55, 1973–1992.

Johnson, C. K. (1965) ORTEP, a Fortran thermal-ellipsoid plot program for crystal structure illustrations. ORNL-3794. (2nd. revision, 1970).

Lager, G. A. and Meagher, E. P. (1978) High-temperature structural study of six olivines. American Mineralogist, 63, 365–377.

Papike, J. J., Ross, M., and Clark, J. R. (1969) Crystal-chemical characterization of clinoamphiboles based on five new structure refinements. Mineralogical Society of America Special Paper, 2, 117–136.

Prewitt, C. T., Sueno, S., and Papike, J. J. (1976) The crystal structures of high albite and monalbite at high temperatures. American Mineralogist, 61, 55–88.

Ribbe, P. H. and Prunier, Jr., A. R. (1977) Stereochemical systematics of ordered C2/c silicate pyroxenes. American Mineralogist, 62, 710–720.

Robinson, K., Gibbs, G. V., and Ribbe, P. H. (1971) Quadratic elongation: a quantitative measure of distortion in coordination polyhedra. Science, 172, 567–570.

Smyth, J. R. and Hazen, R. M. (1973) The crystal structures of forsterite and hortonolite at several temperatures up to 900°C. American Mineralogist, 58, 588–593.

Sueno, S., Cameron, M., and Prewitt, C. T. (1976) Orthoferrosilite: high-temperature crystal chemistry. American Mineralogist, 61, 38–53.

Sueno, S., Cameron, M., Papike, J. J., and Prewitt, C. T. (1973) High-temperature crystal chemistry of tremolite. American Mineralogist, 58, 649–664.

Sueno, S., Papike, J. J., Prewitt, C. T., and Brown, G. E. (1972) The crystal structure of high cummingtonite. Journal of Geophysical Research, 77, 5767–5777.

Winter, J. K., Okamura, F. P., and Ghose, S. (1979) A high-temperature structural study of high-albite, monalbite, and the analbite → monalbite phase transition. American Mineralogist, 64, 409–423.

Appendix

Table A1. Data collection information for richterites

Amphibole	Temperature (°C)	Number of Reflections	R[a] (Anisotropic)	Wtd.R[b] (Anisotropic)
K fluor-richterite KNaCaMg$_5$Si$_8$O$_{22}$F$_2$	24	1182	0.051	0.042
	400	1156	0.061	0.045
	600	1133	0.067	0.047
	800	1141	0.072	0.046
Na fluor-richterite NaNaCaMg$_5$Si$_8$O$_{22}$F$_2$	24	1191	0.037	0.034
	400	1202	0.045	0.039
	600	1191	0.054	0.042
	800	1190	0.057	0.043
	900	1158	0.078	0.063

[a] $R = \Sigma||F_o| - |F_c||/\Sigma|F_o|$

[b] $\text{Wtd.R} = [\Sigma W(|F_o| - |F_c|)^2/\Sigma W|F_o|^2]^{1/2}$

Table A2. Final positional parameters (*I2/m* space group) and equivalent isotropic temperature factors for richterites

Atom	Parameter	K fluor-richterite 24°C	400°C	600°C	800°C	Na fluor-richterite 24°C	400°C	600°C	800°C	900°C
O1	x	0.1112(2)[a]	0.1112(3)	0.1104(3)	0.1108(3)	0.1132(1)	0.1132(2)	0.1131(2)	0.1131(2)	0.1129(3)
	y	0.9150(1)	0.9147(1)	0.9147(1)	0.9146(1)	0.9157(1)	0.9157(1)	0.9156(1)	0.9152(1)	0.9152(2)
	z	0.8919(4)	0.8918(5)	0.8914(5)	0.8910(5)	0.8951(3)	0.8953(3)	0.8954(4)	0.8952(4)	0.8954(7)
	B	0.49(3)	1.06(4)	1.38(5)	1.69(5)	0.55(2)	0.98(3)	1.23(3)	1.51(4)	1.70(6)
O2	x	0.1180(2)	0.1180(3)	0.1186(3)	0.1193(3)	0.1188(1)	0.1192(2)	0.1191(2)	0.1196(2)	0.1196(3)
	y	0.8314(1)	0.8310(1)	0.8308(1)	0.8306(2)	0.8324(1)	0.8324(1)	0.8323(1)	0.8322(1)	0.8320(2)
	z	0.3918(4)	0.3924(5)	0.3923(5)	0.3926(5)	0.3922(3)	0.3923(3)	0.3922(4)	0.3918(4)	0.3919(7)
	B	0.57(3)	1.18(4)	1.37(5)	1.79(5)	0.60(2)	1.13(3)	1.43(3)	1.67(4)	1.93(6)
O3	x	0.1015(3)	0.1018(3)	0.1025(4)	0.1014(4)	0.1031(2)	0.1029(2)	0.1033(3)	0.1031(3)	0.1029(5)
	y	0.0	0.0	0.0	0.0	0.0	0.0	0.0	0.0	0.0
	z	0.3875(5)	0.3877(6)	0.3874(7)	0.3884(7)	0.3910(3)	0.3907(4)	0.3909(5)	0.3915(6)	0.3923(9)
	B	0.73(4)	1.58(6)	1.94(6)	2.52(7)	0.72(3)	1.47(4)	1.88(5)	2.36(5)	2.69(9)
O4	x	0.3610(2)	0.3608(3)	0.3615(3)	0.3613(3)	0.3613(2)	0.3614(2)	0.3619(2)	0.3618(3)	0.3625(4)
	y	0.7515(1)	0.7522(1)	0.7531(2)	0.7537(2)	0.7510(1)	0.7521(1)	0.7526(1)	0.7534(1)	0.7533(2)
	z	0.5641(5)	0.5605(5)	0.5593(7)	0.5591(6)	0.5678(3)	0.5650(4)	0.5641(5)	0.5629(5)	0.5650(8)
	B	0.78(4)	1.60(5)	2.05(6)	2.47(6)	0.79(2)	1.51(3)	1.90(4)	2.31(5)	2.56(8)
O5	x	0.3454(2)	0.3437(3)	0.3432(3)	0.3420(3)	0.3492(1)	0.3476(2)	0.3472(2)	0.3460(2)	0.3462(4)
	y	0.8697(1)	0.8708(1)	0.8717(2)	0.8722(2)	0.8694(1)	0.8709(1)	0.8717(1)	0.8723(1)	0.8725(2)
	z	0.2496(4)	0.2506(5)	0.2502(6)	0.2511(6)	0.2585(3)	0.2601(5)	0.2603(5)	0.2603(5)	0.2623(7)
	B	0.74(4)	1.32(4)	1.71(5)	2.14(5)	0.75(2)	1.43(3)	1.74(4)	2.13(4)	2.33(7)
O6	x	0.3418(2)	0.3404(3)	0.3396(3)	0.3387(3)	0.3448(1)	0.3439(2)	0.3433(2)	0.3427(2)	0.3422(4)
	y	0.8826(1)	0.8820(1)	0.8819(2)	0.8814(2)	0.8831(1)	0.8821(1)	0.8822(1)	0.8819(1)	0.8814(2)
	z	0.7486(4)	0.7503(5)	0.7518(6)	0.7514(5)	0.7562(3)	0.7597(3)	0.7600(4)	0.7606(4)	0.7602(7)
	B	0.71(4)	1.41(5)	1.71(5)	2.09(5)	0.76(2)	1.39(3)	1.77(4)	2.10(4)	2.37(7)
O7	x	0.3359(3)	0.3343(4)	0.3331(5)	0.3315(5)	0.3436(2)	0.3419(3)	0.3413(3)	0.3402(4)	0.3403(6)
	y	0.0	0.0	0.0	0.0	0.0	0.0	0.0	0.0	0.0
	z	0.0328(7)	0.0297(8)	0.0287(9)	0.0264(9)	0.0540(4)	0.0487(5)	0.0457(7)	0.0441(7)	0.0418(11)
	B	0.78(5)	1.55(7)	1.86(8)	2.25(8)	0.75(3)	1.50(4)	1.85(5)	2.17(6)	2.51(10)
T1	x	0.2772(1)	0.2762(1)	0.2754(1)	0.2749(1)	0.2813(1)	0.2804(1)	0.2799(1)	0.2794(1)	0.2794(1)
	y	0.9152(1)	0.9155(1)	0.9155(1)	0.9157(1)	0.9156(1)	0.9159(1)	0.9159(1)	0.9161(1)	0.9162(1)
	z	0.9769(2)	0.9770(2)	0.9769(2)	0.9768(2)	0.9860(1)	0.9858(1)	0.9857(2)	0.9856(2)	0.9857(3)
	B	0.41(1)	0.78(2)	0.97(2)	1.25(2)	0.40(1)	0.77(1)	0.96(1)	1.15(2)	1.35(2)
T2	x	0.2858(1)	0.2854(1)	0.2851(1)	0.2848(1)	0.2875(1)	0.2872(1)	0.2871(1)	0.2869(1)	0.2870(1)
	y	0.8285(1)	0.8289(1)	0.8291(1)	0.8293(1)	0.8289(1)	0.8294(1)	0.8296(1)	0.8298(1)	0.8299(1)
	z	0.4805(2)	0.4807(2)	0.4806(2)	0.4805(2)	0.4863(1)	0.4867(1)	0.4866(2)	0.4867(2)	0.4874(3)
	B	0.41(1)	0.80(2)	1.04(2)	1.28(2)	0.43(1)	0.85(1)	1.03(1)	1.25(2)	1.44(2)
M1	x	0.0	0.0	0.0	0.0	0.0	0.0	0.0	0.0	0.0
	y	0.9107(1)	0.9102(1)	0.9100(1)	0.9098(1)	0.9112(1)	0.9109(1)	0.9107(1)	0.9105(1)	0.9104(1)
	z	0.5	0.5	0.5	0.5	0.5	0.5	0.5	0.5	0.5
	B	0.47(2)	1.01(3)	1.34(3)	1.66(4)	0.51(2)	1.02(2)	1.28(2)	1.55(3)	1.80(4)
M2	x	0.0	0.0	0.0	0.0	0.0	0.0	0.0	0.0	0.0
	y	0.8210(1)	0.8202(1)	0.8197(1)	0.8191(1)	0.8212(1)	0.8206(1)	0.8202(1)	0.8196(1)	0.8194(1)
	z	0.0	0.0	0.0	0.0	0.0	0.0	0.0	0.0	0.0
	B	0.61(3)	1.14(3)	1.41(3)	1.89(4)	0.59(2)	1.10(2)	1.42(3)	1.72(3)	1.93(4)
M3	x	0.0	0.0	0.0	0.0	0.0	0.0	0.0	0.0	0.0
	y	0.0	0.0	0.0	0.0	0.0	0.0	0.0	0.0	0.0
	z	0.0	0.0	0.0	0.0	0.0	0.0	0.0	0.0	0.0
	B	0.53(3)	0.99(4)	1.20(4)	1.68(5)	0.47(2)	0.93(3)	1.19(3)	1.53(4)	1.75(6)
M4	x	0.0	0.0	0.0	0.0	0.0	0.0	0.0	0.0	0.0
	y	0.7227(1)	0.7222(1)	0.7217(1)	0.7216(1)	0.7243(1)	0.7239(1)	0.7236(1)	0.7235(1)	0.7235(1)
	z	0.5	0.5	0.5	0.5	0.5	0.5	0.5	0.5	0.5
	B	0.83(2)	1.94(3)	2.54(4)	3.18(4)	0.97(1)	2.04(2)	2.65(3)	3.23(3)	3.60(5)
A	x	0.485(7)	0.482(4)	0.476(1)	0.475(2)	0.4756(9)	0.472(1)	0.470(2)	0.469(2)	0.467(3)
	y	0.0	0.0	0.0	0.0	0.9868(4)	0.988(1)	0.991(3)	0.989(2)	
	z	0.508(16)	0.525(9)	0.527(4)	0.533(4)	0.5365(17)	0.540(3)	0.543(3)	0.548(3)	0.553(5)
	B	4.2(6)	5.9(5)	5.8(3)	6.7(3)	3.7(2)	6.4(5)	7.2(6)	9.1(9)	10.2(1.1)

[a] Error in parentheses represents one standard deviation.

Table A3. Interatomic distances (Å) in tetrahedral chains of richterites

Atom	K fluor-richterite				Na fluor-richterite				
	24°C	400°C	600°C	800°C	24°C	400°C	600°C	800°C	900°C
T1 Tetrahedron									
T1-O1	1.595(2)[a]	1.594(3)	1.598(3)	1.595(3)	1.601(1)	1.598(2)	1.599(2)	1.597(2)	1.602(3)
T1-O5	1.630(2)	1.631(3)	1.625(3)	1.628(3)	1.626(1)	1.624(2)	1.623(2)	1.621(2)	1.629(4)
T1-O6	1.619(2)	1.622(3)	1.619(3)	1.626(3)	1.623(1)	1.620(2)	1.622(2)	1.623(2)	1.627(4)
T1-O7	1.631(1)	1.629(3)	1.633(2)	1.630(2)	1.637(1)	1.635(1)	1.636(1)	1.635(1)	1.634(2)
Mean	1.619	1.619	1.619	1.620	1.622	1.619	1.620	1.619	1.623
Q.E.[b]	1.0026	1.0023	1.0025	1.0021	1.0028	1.0025	1.0027	1.0024	1.0023
O1-O5	2.698(3)	2.692(4)	2.696(4)	2.692(4)	2.698(2)	2.689(2)	2.691(3)	2.683(3)	2.691(5)
O1-O6	2.675(3)	2.672(4)	2.674(4)	2.671(4)	2.671(2)	2.668(2)	2.670(3)	2.667(3)	2.671(5)
O1-O7	2.649(3)	2.652(4)	2.655(4)	2.649(4)	2.671(2)	2.667(3)	2.671(3)	2.672(3)	2.677(5)
O5-O6	2.636(3)	2.637(4)	2.627(4)	2.638(4)	2.640(2)	2.634(2)	2.637(3)	2.637(3)	2.648(5)
O5-O7	2.595(3)	2.598(3)	2.591(3)	2.596(3)	2.573(2)	2.574(2)	2.576(3)	2.576(3)	2.585(4)
O6-O7	2.596(3)	2.600(3)	2.601(4)	2.610(4)	2.621(2)	2.618(2)	2.614(3)	2.617(3)	2.621(5)
Mean	2.642	2.642	2.641	2.643	2.646	2.642	2.643	2.642	2.649
T2 Tetrahedron									
T2-O2	1.614(2)	1.618(3)	1.613(3)	1.609(3)	1.608(1)	1.607(2)	1.611(2)	1.608(2)	1.611(3)
T2-O4	1.579(2)	1.579(3)	1.576(3)	1.575(3)	1.580(1)	1.577(2)	1.578(2)	1.573(2)	1.579(4)
T2-O5	1.665(2)	1.665(3)	1.674(3)	1.672(3)	1.661(2)	1.663(2)	1.668(2)	1.668(2)	1.665(4)
T2-O6	1.679(2)	1.678(3)	1.684(3)	1.678(3)	1.680(2)	1.681(2)	1.684(2)	1.684(2)	1.673(4)
Mean	1.634	1.635	1.637	1.634	1.632	1.632	1.635	1.633	1.632
Q.E.	1.0069	1.0064	1.0068	1.0069	1.0060	1.0060	1.0062	1.0063	1.0063
O2-O4	2.753(3)	2.752(4)	2.750(4)	2.744(4)	2.742(2)	2.740(2)	2.746(3)	2.739(3)	2.747(5)
O2-O5	2.669(3)	2.671(4)	2.674(4)	2.668(4)	2.665(2)	2.660(2)	2.667(3)	2.660(3)	2.661(5)
O2-O6	2.662(3)	2.664(4)	2.665(4)	2.658(4)	2.660(2)	2.662(2)	2.667(3)	2.667(3)	2.663(5)
O4-O5	2.671(3)	2.670(4)	2.672(4)	2.673(4)	2.658(2)	2.659(2)	2.664(3)	2.661(3)	2.667(5)
O4-O6	2.576(3)	2.579(4)	2.577(4)	2.567(4)	2.593(2)	2.586(2)	2.589(3)	2.583(3)	2.574(5)
O5-O6	2.645(3)	2.651(4)	2.664(4)	2.659(4)	2.641(2)	2.651(2)	2.655(3)	2.659(3)	2.649(5)
Mean	2.663	2.665	2.667	2.662	2.660	2.660	2.665	2.662	2.660

[a] Error in parentheses represents one standard deviation.
[b] Quadratic elongation of Robinson et al. (1971).

Table A4. Interatomic angles (°) in tetrahedral chains of richterites

Atoms	K fluor-richterite				Na fluor-richterite				
	24°C	400°C	600°C	800°	24°C	400°C	600°C	800°C	900°C
T1 Tetrahedron									
O1-T1-O5	113.5(1)[a]	113.2(2)	113.5(2)	113.3(2)	113.5(1)	113.1(1)	113.2(1)	113.0(1)	112.8(2)
O1-T1-O6	112.6(1)	112.4(1)	112.5(2)	112.1(2)	111.9(1)	112.0(1)	112.0(1)	111.8(1)	111.6(2)
O1-T1-O7	110.3(1)	110.7(2)	110.6(2)	110.5(2)	111.2(1)	111.2(1)	111.3(1)	111.5(1)	111.6(2)
O5-T1-O6	108.4(1)	108.3(2)	108.2(2)	108.3(2)	108.7(1)	108.6(1)	108.7(1)	108.7(1)	108.8(2)
O5-T1-O7	105.4(1)	105.7(2)	105.4(2)	105.7(2)	104.1(1)	104.3(1)	104.4(1)	104.6(2)	104.7(3)
O6-T1-O7	106.0(2)	106.2(2)	106.3(2)	106.6(2)	107.0(1)	107.1(1)	106.7(1)	106.9(2)	106.9(3)
Mean	109.4	109.4	109.4	109.4	109.4	109.4	109.4	109.4	109.4
T2 Tetrahedron									
O2-T2-O4	119.1(1)	118.8(2)	119.1(2)	119.1(2)	118.7(1)	118.7(1)	118.9(1)	118.9(1)	118.9(2)
O2-T2-O5	109.0(1)	108.9(1)	108.9(2)	108.8(2)	109.2(1)	108.9(1)	108.9(1)	108.6(1)	108.6(2)
O2-T2-O6	107.8(1)	107.8(1)	107.8(2)	107.9(2)	108.0(1)	108.0(1)	108.0(1)	108.2(1)	108.3(2)
O4-T2-O5	110.8(1)	110.8(2)	110.6(2)	110.8(2)	110.2(1)	110.3(1)	110.3(1)	110.4(1)	110.5(2)
O4-T2-O6	104.4(1)	104.6(2)	104.4(2)	104.2(2)	105.4(1)	105.1(1)	105.0(1)	104.9(1)	104.6(2)
O5-T2-O6	104.6(1)	104.9(1)	105.0(2)	105.1(2)	104.5(1)	104.9(1)	104.8(1)	105.0(1)	105.0(2)
Mean	109.3	109.3	109.3	109.3	109.3	109.3	109.3	109.3	109.3
T1-O5-T2	135.9(2)	136.5(2)	136.4(2)	136.8(2)	135.5(1)	136.2(1)	136.2(1)	136.7(2)	136.7(3)
T1-O6-T2	136.3(2)	137.1(2)	137.3(2)	137.8(2)	136.7(1)	137.3(1)	137.5(1)	137.8(2)	138.2(3)
T1-O7-T1	138.3(2)	138.7(3)	139.1(3)	139.8(3)	135.5(1)	136.3(2)	136.6(2)	137.0(2)	137.1(4)
O5-O6-O5	169.8(1)	171.1(2)	171.8(2)	172.6(2)	169.2(1)	171.1(1)	171.6(1)	172.3(1)	172.8(2)
O5-O7-O6	169.3(2)	170.5(2)	170.8(2)	171.3(2)	167.5(1)	169.4(1)	170.1(1)	170.7(2)	171.5(3)

[a] Error in parentheses represents one standard deviation.

Table A5. Interatomic distances (Å) in M polyhedra of richterites

Atoms[a]	K fluor-richterite				Na fluor-richterite				
	24°C	400°C	600°C	800°C	24°C	400°C	600°C	800°C	900°C
M1 Octahedron									
M1-O1 [2][b]	2.060(2)[c]	2.064(2)	2.064(3)	2.066(3)	2.062(1)	2.066(2)	2.070(2)	2.072(2)	2.074(3)
M1-O2 [2]	2.027(2)	2.034(3)	2.044(3)	2.053(3)	2.025(1)	2.031(2)	2.036(2)	2.043(2)	2.046(4)
M1-O3 [2]	2.070(2)	2.087(2)	2.100(3)	2.100(3)	2.063(1)	2.076(2)	2.085(2)	2.091(2)	2.091(3)
Mean	2.052	2.062	2.069	2.073	2.050	2.058	2.064	2.069	2.070
Volume[d]	11.299	11.453	11.579	11.647	11.273	11.405	11.507	11.587	11.612
Q.E.[e]	1.0135	1.0134	1.0132	1.0134	1.0127	1.0128	1.0128	1.0127	1.0129
O1u-O2u [2]	3.046(3)	3.053(4)	3.061(4)	3.065(4)	3.053(2)	3.062(2)	3.069(3)	3.073(3)	3.077(5)
O1u-O3u [2]	3.040(3)	3.051(4)	3.058(4)	3.055(4)	3.029(2)	3.040(2)	3.046(3)	3.050(3)	3.049(5)
O2-O3 [2]	3.035(2)	3.056(3)	3.067(3)	3.081(3)	3.014(1)	3.027(7)	3.037(2)	3.047(2)	3.053(4)
O1u-O2d [2oo]	2.805(3)	2.819(3)	2.826(4)	2.841(4)	2.801(2)	2.812(2)	2.819(3)	2.826(3)	2.828(4)
O1u-O3d [2oo]	2.704(3)	2.720(3)	2.726(4)	2.730(4)	2.706(2)	2.714(2)	2.725(3)	2.734(3)	2.736(5)
O2-O2 [1op]	2.884(4)	2.894(5)	2.913(6)	2.931(6)	2.897(3)	2.915(6)	2.922(4)	2.940(4)	2.941(7)
O3-O3 [1oo]	2.612(5)	2.628(7)	2.649(7)	2.628(8)	2.618(3)	2.629(4)	2.640(5)	2.637(6)	2.630(9)
Mean	2.896	2.910	2.920	2.925	2.893	2.905	2.913	2.920	2.921
M2 Octahedron									
M2-O1 [2]	2.181(2)	2.199(3)	2.208(3)	2.223(3)	2.192(2)	2.209(2)	2.219(2)	2.227(2)	2.230(4)
M2-O2 [2]	2.085(2)	2.094(2)	2.099(3)	2.106(3)	2.072(1)	2.079(2)	2.083(2)	2.086(2)	2.087(3)
M2-O4 [2]	1.998(2)	2.002(3)	2.005(3)	2.013(3)	1.997(2)	2.005(2)	2.006(2)	2.013(3)	2.010(4)
Mean	2.088	2.098	2.104	2.114	2.087	2.098	2.103	2.109	2.109
Volume	11.940	12.086	12.173	12.351	11.919	12.094	12.172	12.263	12.276
Q.E.	1.0127	1.0137	1.0144	1.0148	1.0127	1.0134	1.0139	1.0144	1.0145
O1u-O2u [2]	3.014(3)	3.026(4)	3.030(4)	3.040(4)	2.999(2)	3.005(2)	3.009(3)	3.010(3)	3.011(5)
O2u-O4u [2]	2.878(3)	2.878(4)	2.880(4)	2.888(4)	2.898(2)	2.905(2)	2.909(3)	2.911(3)	2.918(5)
O4-O4 [1]	3.032(5)	3.033(6)	3.021(7)	3.033(7)	3.038(3)	3.035(4)	3.028(5)	3.031(5)	3.031(8)
O1-O4 [2]	3.007(3)	3.031(4)	3.057(4)	3.074(4)	3.005(2)	3.038(2)	3.055(3)	3.071(3)	3.070(5)
O1u-O2d [2oo]	2.805(3)	2.819(3)	2.826(4)	2.841(4)	2.801(2)	2.812(2)	2.819(3)	2.826(3)	2.828(4)
O2u-O4d [2op]	3.061(3)	3.087(4)	3.102(4)	3.120(4)	3.033(2)	3.060(2)	3.070(3)	3.088(3)	3.080(5)
O1u-O1d [1oo]	2.759(4)	2.771(5)	2.767(6)	2.785(5)	2.774(3)	2.785(3)	2.789(4)	2.797(4)	2.793(6)
Mean	2.943	2.957	2.965	2.979	2.940	2.955	2.962	2.970	2.970
M3 Octahedron									
M3-O1 [4]	2.059(2)	2.071(2)	2.073(3)	2.084(3)	2.052(1)	2.062(2)	2.068(2)	2.078(2)	2.079(3)
M3-O3 [2]	2.014(3)	2.021(3)	2.023(3)	2.029(3)	2.018(3)	2.019(2)	2.025(3)	2.030(3)	2.034(5)
Mean	2.044	2.054	2.056	2.066	2.041	2.048	2.054	2.062	2.064
Volume	11.133	11.314	11.351	11.490	11.127	11.232	11.332	11.467	11.490
Q.E.	1.0144	1.0144	1.0144	1.0150	1.0127	1.0128	1.0126	1.0131	1.0133
O1u-O1u [2]	3.056(4)	3.080(5)	3.089(5)	3.102(5)	3.025(3)	3.042(3)	3.054(4)	3.073(4)	3.079(6)
O1u-O3u [4]	3.046(3)	3.058(4)	3.059(4)	3.077(4)	3.041(2)	3.048(2)	3.054(3)	3.066(3)	3.071(5)
O1u-O1d [2oo]	2.759(4)	2.771(5)	2.767(6)	2.785(5)	2.774(3)	2.785(3)	2.789(4)	2.797(4)	2.793(6)
O1u-O3d [4oo]	2.704(3)	2.720(3)	2.726(4)	2.730(4)	2.706(2)	2.715(2)	2.725(3)	2.734(3)	2.736(5)
Mean	2.886	2.901	2.904	2.917	2.882	2.892	2.900	2.912	2.914
M4 Polyhedron									
M4-O2 [2]	2.427(2)	2.440(3)	2.455(3)	2.463(3)	2.421(2)	2.440(2)	2.450(2)	2.459(3)	2.459(4)
M4-O4 [2]	2.380(2)	2.402(3)	2.406(3)	2.411(3)	2.339(2)	2.352(2)	2.358(2)	2.365(3)	2.355(3)
M4-O6 [2]	2.587(2)	2.587(3)	2.587(3)	2.591(3)	2.571(2)	2.561(2)	2.566(2)	2.568(3)	2.566(5)
M4-O5 [2]	2.824(2)	2.856(3)	2.870(3)	2.893(3)	2.844(2)	2.844(2)	2.899(2)	2.917(3)	2.928(4)
Mean for 6	2.465	2.476	2.483	2.488	2.444	2.451	2.458	2.464	2.460
Mean for 8	2.555	2.571	2.580	2.590	2.544	2.559	2.568	2.577	2.577
Volume (Å3)	27.561	28.090	28.304	28.626	27.140	27.597	27.860	28.146	28.105
M1-M1	3.211(3)	3.243(3)	3.258(4)	3.275(4)	3.190(2)	3.215(2)	3.229(3)	3.246(3)	3.252(5)
M1-M2	3.085(1)	3.097(1)	3.105(1)	3.114(1)	3.085(1)	3.098(1)	3.106(1)	3.113(1)	3.117(2)
M1-M3	3.081(1)	3.095(1)	3.101(1)	3.109(1)	3.075(1)	3.087(1)	3.094(1)	3.101(1)	3.103(1)
M1-M4	3.377(2)	3.395(2)	3.410(3)	3.418(3)	3.354(1)	3.371(2)	3.385(2)	3.391(2)	3.393(3)
M2-M3	3.218(1)	3.247(2)	3.265(2)	3.284(2)	3.210(1)	3.236(1)	3.253(1)	3.270(2)	3.278(2)
M2-M4	3.167(1)	3.174(1)	3.180(1)	3.182(2)	3.152(1)	3.159(1)	3.165(1)	3.166(1)	3.165(2)

[a] The superscript notation u = up, d = down refers to oxygen x values greater (u) or less (d) than the x of M.
[b] Number in brackets is the multiplicity of the interatomic distance. Superscript oo indicates an edge shared between two octahedra and superscript op an edge shared between an octahedron and the M4 polyhedron.
[c] Error in parenthesis is one standard deviation.
[d] Volume of polyhedron.
[e] Quadratic elongation parameter of Robinson et al. (1971).

Table A6. Selected interatomic angles (°) in M polyhedra of richterites

Atoms[a]	K fluor-richterite				Na fluor-richterite				
	24°C	400°C	600°C	800°C	24°C	400°C	600°C	800°C	900°C
M1 Octahedron									
O1u-M1-O2u	96.4(1)[b]	96.3(1)	96.4(1)	96.2(1)	96.7(1)	96.7(1)	96.7(1)	96.6(1)	96.6(1)
O1u-M1-O3u	94.8(1)	94.6(1)	94.5(1)	94.3(1)	94.5(1)	94.4(1)	94.3(1)	94.2(1)	94.1(2)
O2-M1-O3	95.6(1)	95.7(1)	95.5(1)	95.8(1)	95.0(1)	94.9(1)	94.9(1)	94.9(1)	95.1(1)
O1u-M1-O2d	86.7(1)	86.9(1)	86.9(1)	87.2(1)	86.5(1)	86.7(7)	86.7(1)	86.7(1)	86.7(1)
O1u-M1-O3d	81.8(1)	81.9(1)	81.8(1)	81.9(1)	82.0(1)	81.9(1)	81.9(1)	82.1(1)	82.1(2)
O2-M1-O2	90.7(1)	90.7(2)	90.9(2)	91.1(2)	91.4(1)	91.7(1)	91.7(1)	92.0(1)	91.9(2)
O3-M1-O3	78.2(1)	78.1(1)	78.2(2)	77.5(2)	78.7(1)	78.5(1)	78.6(1)	78.2(1)	77.9(2)
Mean	90.0	90.0	89.9	90.0	90.0	90.0	90.0	89.9	89.9
M2 Octahedron									
O1u-M2-O2u	89.8(1)	89.6(1)	89.4(1)	89.1(1)	89.3(1)	88.9(1)	88.7(1)	88.5(1)	88.4(1)
O2u-M2-O4u	89.6(9)	89.2(1)	89.1(1)	89.0(1)	90.8(1)	90.7(1)	90.7(1)	90.5(1)	90.8(2)
O4-M2-O4	98.7(2)	98.5(2)	97.8(2)	97.8(2)	99.1(1)	98.4(1)	98.0(2)	97.7(2)	97.9(3)
O1-M2-O4	91.9(1)	92.3(1)	92.9(1)	92.9(1)	91.6(1)	92.1(1)	92.5(1)	92.7(1)	92.7(1)
O1u-M2-O2d	82.2(1)	82.1(1)	82.0(1)	82.0(1)	82.1(1)	81.9(1)	81.8(1)	81.8(1)	81.8(1)
O2u-M2-O4d	97.1(1)	97.8(1)	98.2(1)	98.5(1)	96.4(1)	97.1(1)	97.3(1)	97.8(1)	97.5(2)
O1u-M2-O1d	78.5(1)	78.1(1)	77.6(2)	77.6(2)	78.5(1)	78.1(1)	77.9(1)	77.8(1)	77.6(2)
Mean	89.9	89.9	89.9	89.9	89.8	89.8	89.8	89.8	89.8
M3 Octahedron									
O1u-M3-O1u	95.9(1)	96.0(1)	96.3(2)	96.2(2)	95.0(1)	95.0(1)	95.2(1)	95.4(1)	95.6(2)
O1u-M3-O3u	96.8(1)	96.7(1)	96.6(1)	96.8(1)	96.7(1)	96.6(1)	96.5(1)	96.6(1)	96.6(1)
O1u-M3-O1d	84.2(1)	84.0(1)	83.7(2)	83.8(2)	85.0(1)	85.0(1)	84.8(1)	84.6(1)	84.4(2)
O1u-M3-O3d	83.2(1)	83.3(1)	83.4(1)	83.2(1)	83.3(1)	83.4(1)	83.5(1)	83.4(1)	83.4(1)
Mean	90.0	90.0	90.0	90.0	90.0	90.0	90.0	90.0	90.0

[a] The superscript notation u = up and d = down refers to oxygen $\underline{x}$ values greater (u) or less (d) than the x of u.
[b] Error in parentheses is one standard deviation.

Table A7. Interatomic distances (Å) in A polyhedra of richterites

	24°C	400°C	600°C	800°C	900°C
K fluor-richterite (A = 4i)					
A-O5 [2][a]	2.87(5)[b]	2.89(3)	2.87(1)	2.88(1)	--
A-O5 [2]	2.97(5)	2.96(3)	2.99(1)	2.99(1)	--
A-O6 [2]	3.01(4)	2.98(2)	2.96(1)	2.95(1)	--
A-O6 [2]	3.25(4)	3.35(3)	3.42(1)	3.47(1)	--
A-O7 [1]	2.54(8)	2.63(5)	2.63(2)	2.68(2)	--
A-O7 [1]	2.58(8)	2.56(5)	2.60(2)	2.60(2)	--
A-O7 [1]	3.47(7)	3.38(4)	3.34(2)	3.31(1)	--
Mean (8)	2.85	2.86	2.86	2.87	--
Mean (10)	2.93	2.955	2.97	2.99	--
Mean (11)	2.98	2.99	3.00	3.02	--
Na fluor-richterite (A = 8j)					
A-O5 [1]	2.66(1)	2.67(2)	2.67(3)	2.72(4)	2.69(3)
A-O5 [1]	2.75(1)	2.79(2)	2.79(3)	2.84(4)	2.81(4)
A-O5 [1]	3.05(1)	3.01(2)	3.01(3)	2.98(5)	3.02(4)
A-O5 [1]	3.13(1)	3.12(2)	3.12(3)	3.08(4)	3.13(4)
A-O6 [1]	2.71(1)	2.74(2)	2.73(3)	2.76(4)	2.71(3)
A-O6 [1]	3.06(1)	3.04(2)	3.04(2)	3.00(4)	3.02(3)
A-O6 [1]	3.26(1)	3.35(1)	3.38(2)	3.45(3)	3.47(3)
A-O6 [1]	3.55[c]	3.61	3.64	3.64	3.71
A-O7 [1]	2.39(1)	2.43(1)	2.44(2)	2.44(2)	2.45(3)
A-O7 [1]	2.51(1)	2.55(1)	2.58(2)	2.61(2)	2.64(3)
A-O7 [1]	3.35(1)	3.30(1)	3.27(1)	3.24(1)	3.20(2)
Mean (8)	2.78	2.79	2.80	2.80	2.81
Mean (10)	2.91	2.93	2.94	2.95	2.965
Mean (11)	2.95	2.96	2.97	2.98	2.99

[a] Number in brackets is the multiplicity of the interatomic distance.
[b] Error in parentheses is one standard deviation.
[c] Distances calculated by hand.

Table A8. Magnitude and orientation of the principal axes of the thermal ellipsoids in K fluor-richterite ($I2/m$ space group)

Atom	Ellipsoid Axis	24°C rms Amplitude	a	b	c	400°C rms Amplitude	a	b	c
O1	r1	0.067(7)[a]	33(14)	123(14)	104(20)	0.101(6)	38(15)	102(18)	70(21)
	r2	0.081(6)	101(26)	106(34)	149(34)	0.111(5)	72(22)	132(12)	137(16)
	r3	0.088(6)	121(15)	142(21)	63(36)	0.134(5)	122(8)	135(10)	53(10)
O2	r1	0.077(7)	148(118)	78(40)	45(101)	0.106(6)	64(31)	76(12)	44(27)
	r2	0.079(6)	122(118)	109(28)	127(104)	0.114(6)	29(29)	109(11)	126(28)
	r3	0.099(5)	90(12)	158(13)	69(12)	0.143(5)	102(7)	156(7)	67(7)
O3	r1	0.078(8)	61(8)	90	45(8)	0.123(6)	58(11)	90	47(11)
	r2	0.093(6)	90	180	90	0.148(6)	32(11)	90	137(11)
	r3	0.113(6)	151(8)	90	45(8)	0.151(5)	90	0	90
O4	r1	0.063(8)	48(4)	137(4)	97(9)	0.092(7)	55(3)	140(3)	84(4)
	r2	0.095(6)	92(7)	97(8)	161(7)	0.151(5)	80(8)	102(7)	167(9)
	r3	0.129(6)	137(4)	132(4)	72(6)	0.172(5)	37(4)	53(4)	102(11)
O5	r1	0.079(7)	105(16)	119(7)	29(8)	0.103(6)	91(9)	121(5)	34(5)
	r2	0.094(5)	156(14)	100(13)	96(16)	0.129(5)	162(9)	105(9)	85(9)
	r3	0.114(5)	109(11)	31(8)	62(7)	0.152(5)	108(9)	35(6)	57(5)
O6	r1	0.078(6)	96(46)	55(6)	36(12)	0.099(6)	101(8)	64(4)	27(4)
	r2	0.084(6)	171(31)	88(28)	83(38)	0.129(5)	167(8)	88(7)	87(8)
	r3	0.118(5)	96(7)	145(6)	55(6)	0.164(4)	97(6)	154(4)	64(4)
O7	r1	0.062(11)	90	0	90	0.095(9)	90	0	90
	r2	0.094(8)	130(9)	90	124(9)	0.137(7)	139(7)	90	115(7)
	r3	0.129(7)	140(9)	90	34(9)	0.177(6)	131(7)	90	25(7)
T1	r1	0.062(3)	54(7)	142(9)	91(10)	0.095(2)	132(16)	67(23)	38(29)
	r2	0.072(3)	110(2)	115(12)	136(13)	0.099(2)	107(25)	49(24)	126(30)
	r3	0.081(3)	137(8)	116(8)	46(13)	0.104(2)	46(14)	50(19)	83(16)
T2	r1	0.061(3)	64(9)	93(7)	42(9)	0.091(2)	57(7)	113(8)	56(10)
	r2	0.074(3)	38(19)	116(26)	128(12)	0.101(2)	63(10)	127(11)	139(11)
	r3	0.078(2)	115(23)	153(25)	75(17)	0.110(2)	135(8)	134(9)	71(9)
M1	r1	0.063(6)	109(11)	90	3(11)	0.106(4)	90(12)	90	16(12)
	r2	0.083(4)	90	180	90	0.113(4)	90	180	90
	r3	0.083(4)	19(11)	90	87(11)	0.120(4)	0(12)	90	106(12)
M2	r1	0.077(4)	90	0	90	0.110(4)	53(8)	90	53(8)
	r2	0.085(4)	135(11)	90	119(11)	0.119(4)	90	180	90
	r3	0.101(4)	135(11)	90	29(11)	0.131(4)	142(8)	90	37(8)
M3	r1	0.070(7)	90	0	90	0.104(7)	92(11)	90	14(11)
	r2	0.080(6)	134(19)	90	120(19)	0.105(7)	90	180	90
	r3	0.093(6)	136(19)	90	30(19)	0.126(5)	2(11)	90	104(11)
M4	r1	0.075(4)	73(2)	90	33(2)	0.118(3)	69(1)	90	37(1)
	r2	0.085(3)	90	180	90	0.132(3)	90	180	90
	r3	0.136(2)	163(2)	90	57(2)	0.206(3)	159(1)	90	53(1)
A	r1	0.114(15)	56(9)	90	49(9)	0.151(4)	63(6)	90	43(6)
	r2	0.185(3)	90	180	90	0.223(4)	90	180	90
	r3	0.335(35)	146(9)	90	41(9)	0.388(27)	153(6)	90	47(6)

Table A8. (continued)

Atom	Ellipsoid Axis	600°C				800°C			
		rms Amplitude	Angles, degrees with respect to a	b	c	rms Amplitude	Angles, degrees with respect to a	b	c
O1	r1	0.117(6)	72(28)	72(20)	39(17)	0.134(6)	14(10)	104(11)	103(11)
	r2	0.125(6)	36(19)	125(14)	108(27)	0.143(5)	95(25)	117(14)	146(15)
	r3	0.152(5)	120(8)	139(8)	57(7)	0.160(5)	103(9)	149(12)	60(13)
O2	r1	0.115(5)	60(964)	84(334)	46(908)	0.126(6)	30(7)	108(7)	82(12)
	r2	0.115(5)	46(905)	110(23)	143(822)	0.144(5)	77(12)	117(8)	153(7)
	r3	0.161(5)	104(5)	160(5)	72(5)	0.177(5)	116(5)	147(6)	65(6)
O3	r1	0.133(7)	83(8)	90	23(8)	0.157(6)	64(6)	90	42(6)
	r2	0.166(6)	90	180	90	0.174(6)	90	180	90
	r3	0.169(6)	173(8)	90	67(8)	0.202(6)	154(6)	90	48(6)
O4	r1	0.118(6)	61(3)	149(3)	89(6)	0.126(6)	64(3)	151(3)	85(5)
	r2	0.160(5)	81(6)	95(6)	172(6)	0.176(5)	83(5)	100(5)	167(6)
	r3	0.196(5)	31(3)	60(3)	98(6)	0.216(5)	27(3)	63(3)	102(5)
O5	r1	0.114(6)	81(11)	117(4)	37(8)	0.125(5)	92(7)	119(3)	32(4)
	r2	0.138(6)	9(11)	84(7)	113(10)	0.161(5)	173(6)	95(6)	79(6)
	r3	0.181(5)	93(5)	28(4)	62(4)	0.199(4)	97(6)	29(3)	61(3)
O6	r1	0.102(7)	108(6)	65(3)	25(3)	0.127(6)	110(8)	60(3)	31(3)
	r2	0.144(6)	161(6)	102(6)	89(6)	0.155(6)	160(8)	99(6)	92(8)
	r3	0.185(5)	86(5)	152(3)	65(3)	0.198(4)	92(5)	149(3)	59(3)
O7	r1	0.110(8)	90	0	90	0.126(8)	90	0	90
	r2	0.150(7)	148(8)	90	106(8)	0.172(7)	145(11)	90	109(11)
	r3	0.189(7)	122(8)	90	16(8)	0.200(7)	125(11)	90	19(11)
T1	r1	0.103(2)	65(8)	84(13)	41(7)	0.121(2)	48(7)	135(21)	88(43)
	r2	0.111(2)	106(16)	16(16)	85(15)	0.123(2)	90(31)	108(35)	156(9)
	r3	0.117(2)	150(11)	104(17)	49(7)	0.134(2)	138(7)	129(7)	66(8)
T2	r1	0.104(2)	71(11)	117(9)	45(14)	0.118(2)	65(10)	111(10)	47(14)
	r2	0.111(2)	48(8)	120(9)	135(14)	0.125(2)	54(9)	127(9)	133(14)
	r3	0.128(2)	49(5)	43(5)	93(5)	0.138(2)	134(6)	136(6)	76(6)
M1	r1	0.123(4)	89(17)	90	17(17)	0.132(4)	93(7)	90	13(7)
	r2	0.133(4)	179(17)	90	73(17)	0.146(3)	90	180	90
	r3	0.135(4)	90	0	90	0.155(4)	3(7)	90	103(7)
M2	r1	0.119(4)	61(6)	90	45(6)	0.146(3)	61(10)	90	45(10)
	r2	0.131(4)	90	180	90	0.155(4)	90	180	90
	r3	0.149(4)	151(6)	90	45(6)	0.162(4)	151(10)	90	45(10)
M3	r1	0.107(6)	121(8)	90	15(8)	0.133(5)	122(8)	90	16(8)
	r2	0.123(5)	90	180	90	0.142(5)	90	180	90
	r3	0.138(5)	31(8)	90	75(8)	0.161(5)	32(8)	90	74(8)
M4	r1	0.134(3)	67(1)	90	39(1)	0.151(3)	68(1)	90	38(1)
	r2	0.152(3)	90	180	90	0.169(3)	90	180	90
	r3	0.235(3)	157(1)	90	51(1)	0.263(3)	158(1)	90	52(1)
A	r1	0.173(7)	57(5)	90	49(5)	0.193(5)	60(5)	90	46(5)
	r2	0.237(4)	90	180	90	0.266(5)	90	180	90
	r3	0.364(17)	147(5)	90	41(5)	0.382(17)	150(5)	90	44(5)

[a] Error in parentheses represents one standard deviation.

Table A9. Magnitude and orientation of the principal axes of the thermal ellipsoids in Na fluor-richterite (*I2/m* space group)

Atom	Ellipsoid Axis	24°C rms Amplitude	Angles, degrees with respect to a	b	c	400°C rms Amplitude	Angles, degrees with respect to a	b	c
O1	r1	0.078(4)[a]	21(30)	80(70)	88(16)	0.102(4)	49(20)	88(16)	58(19)
	r2	0.081(4)	98(66)	12(62)	96(17)	0.108(4)	53(21)	129(11)	130(19)
	r3	0.090(4)	109(15)	84(17)	6(17)	0.123(3)	118(9)	140(11)	56(10)
O2	r1	0.078(4)	95(34)	65(10)	27(11)	0.106(4)	18(21)	101(15)	92(36)
	r2	0.083(4)	166(16)	80(18)	84(32)	0.110(4)	81(38)	111(9)	158(6)
	r3	0.099(3)	103(10)	153(8)	64(8)	0.140(3)	105(4)	156(5)	68(5)
O3	r1	0.085(5)	72(7)	90	34(7)	0.129(4)	90	0	90
	r2	0.091(4)	90	180	90	0.132(4)	96(11)	90	157(11)
	r3	0.110(4)	162(7)	90	56(7)	0.148(4)	174(11)	90	67(11)
O4	r1	0.080(4)	61(5)	146(4)	83(11)	0.104(4)	63(3)	146(3)	80(5)
	r2	0.095(4)	72(7)	98(10)	172(11)	0.133(4)	75(4)	102(5)	168(5)
	r3	0.121(3)	35(4)	58(4)	93(6)	0.169(3)	32(3)	59(2)	98(4)
O5	r1	0.079(4)	106(15)	124(4)	34(4)	0.096(4)	91(5)	122(2)	35(3)
	r2	0.091(4)	162(14)	88(9)	91(13)	0.128(3)	172(3)	96(4)	79(5)
	r2	0.119(3)	98(5)	34(4)	56(4)	0.170(3)	98(3)	33(2)	57(2)
O6	r1	0.073(4)	106(6)	58(4)	32(4)	0.091(4)	106(4)	63(2)	27(2)
	r2	0.100(3)	163(7)	103(8)	85(7)	0.132(3)	164(4)	97(4)	87(4)
	r3	0.117(3)	86(8)	145(5)	59(4)	0.164(3)	90(4)	152(2)	63(2)
O7	r1	0.072(6)	90	0	90	0.093(6)	90	0	90
	r2	0.095(5)	146(9)	90	107(9)	0.131(5)	157(5)	90	96(5)
	r3	0.118(4)	124(9)	90	17(9)	0.175(4)	113(5)	90	6(5)
T1	r1	0.068(2)	63(15)	153(15)	99(23)	0.095(2)	111(23)	69(32)	22(38)
	r2	0.071(2)	66(24)	77(23)	165(24)	0.096(2)	121(19)	44(22)	108(44)
	r3	0.074(2)	37(18)	67(13)	78(24)	0.104(2)	38(7)	53(8)	98(6)
T2	r1	0.068(2)	48(13)	129(8)	79(25)	0.095(2)	82(11)	99(10)	26(14)
	r2	0.071(2)	68(19)	100(17)	169(23)	0.099(2)	43(5)	131(5)	114(15)
	r3	0.080(2)	50(6)	41(6)	94(8)	0.115(1)	48(4)	42(4)	100(2)
M1	r1	0.077(3)	121(16)	90	14(16)	0.105(3)	98(8)	90	9(8)
	r2	0.078(3)	90	180	90	0.116(2)	90	180	90
	r3	0.085(3)	31(16)	90	76(16)	0.120(2)	8(7)	90	99(7)
M2	r1	0.084(3)	46(17)	90	61(17)	0.116(2)	67(22)	90	40(22)
	r2	0.085(3)	90	180	90	0.118(2)	90	180	90
	r3	0.091(3)	136(17)	90	29(17)	0.121(2)	157(22)	90	50(22)
M3	r1	0.071(4)	90	0	90	0.101(4)	113(9)	90	7(9)
	r2	0.074(4)	65(16)	90	171(16)	0.103(4)	90	180	90
	r3	0.085(4)	25(16)	90	81(16)	0.120(3)	23(9)	90	83(9)
M4	r1	0.083(2)	71(1)	90	36(1)	0.121(2)	70(1)	90	37(1)
	r2	0.100(2)	90	180	90	0.135(2)	90	180	90
	r3	0.142(2)	161(1)	90	54(1)	0.211(2)	160(1)	90	53(1)
A	r1	0.112(9)	60(3)	74(7)	50(5)	0.139(16)	56(3)	65(5)	59(4)
	r2	0.179(12)	81(5)	26(5)	116(6)	0.253(21)	89(6)	31(6)	120(6)
	r3	0.312(11)	148(3)	70(3)	51(3)	0.400(19)	146(3)	73(6)	46(5)

Table A9. (continued)

Atom	Ellipsoid Axis	600°C rms Amplitude	a	b	c	800°C rms Amplitude	a	b	c	900°C rms Amplitude	a	b	c
			Angles, degrees with respect to				Angles, degrees with respect to				Angles, degrees with respect to		
O1	r1	0.113(4)	31(10)	120(11)	102(13)	0.123(4)	26(7)	103(10)	84(10)	0.126(7)	139(9)	90(9)	32(9)
	r2	0.125(4)	103(15)	118(17)	139(17)	0.138(4)	84(12)	136(12)	133(12)	0.155(6)	109(51)	150(84)	105(42)
	r3	0.135(4)	117(9)	137(13)	51(17)	0.152(4)	115(6)	131(12)	44(12)	0.158(6)	56(34)	120(83)	62(26)
O2	r1	0.119(4)	63(27)	84(12)	44(25)	0.125(4)	60(12)	87(7)	46(12)	0.143(6)	28(94)	96(22)	79(101)
	r2	0.125(4)	33(24)	113(6)	127(26)	0.139(4)	38(11)	116(6)	130(12)	0.146(6)	65(102)	102(14)	165(73)
	r3	0.156(3)	108(5)	156(5)	70(5)	0.168(4)	111(5)	154(6)	70(5)	0.178(6)	101(8)	167(8)	80(8)
O3	r1	0.145(4)	90	0	90	0.163(5)	76(8)	90	31(8)	0.173(7)	90	0	90
	r2	0.151(5)	112(12)	90	141(12)	0.167(4)	90	180	90	0.186(7)	95(40)	90	159(40)
	r3	0.167(4)	158(12)	90	51(12)	0.188(4)	166(8)	90	59(8)	0.194(7)	175(39)	90	69(39)
O4	r1	0.114(4)	62(2)	149(2)	87(5)	0.117(4)	62(2)	151(2)	90(3)	0.132(7)	121(3)	32(4)	73(6)
	r2	0.152(4)	77(4)	96(5)	173(5)	0.172(4)	79(4)	93(4)	174(4)	0.180(6)	75(7)	71(6)	161(6)
	r3	0.190(3)	31(3)	60(2)	96(4)	0.211(4)	30(2)	61(2)	96(4)	0.218(6)	35(4)	65(4)	82(7)
O5	r1	0.111(4)	103(7)	121(2)	31(2)	0.126(4)	91(6)	120(2)	33(4)	0.129(7)	105(8)	118(3)	28(3)
	r2	0.138(4)	166(7)	87(5)	86(6)	0.155(4)	178(4)	91(4)	75(6)	0.164(6)	164(8)	85(6)	88(7)
	r2	0.187(3)	94(3)	31(2)	59(2)	0.202(3)	92(3)	30(2)	61(2)	0.212(5)	93(5)	29(3)	62(3)
O6	r1	0.109(5)	108(5)	59(2)	31(2)	0.114(5)	112(4)	61(2)	30(2)	0.124(7)	113(5)	63(3)	28(3)
	r2	0.146(4)	161(5)	95(4)	91(4)	0.165(4)	157(6)	96(5)	95(4)	0.178(6)	156(5)	94(8)	97(6)
	r3	0.184(3)	95(4)	149(2)	59(2)	0.199(3)	96(4)	150(4)	60(2)	0.207(5)	98(8)	153(3)	63(3)
O7	r1	0.106(6)	90	0	90	0.114(6)	90	0	90	0.128(9)	90	0	90
	r2	0.146(5)	154(5)	90	99(5)	0.164(5)	150(6)	90	103(6)	0.176(8)	155(9)	90	98(9)
	r3	0.194(5)	116(5)	90	9(5)	0.206(5)	120(6)	90	13(6)	0.219(8)	115(9)	90	8(9)
T1	r1	0.105(2)	118(8)	58(11)	36(14)	0.115(2)	119(7)	42(8)	55(10)	0.116(3)	137(5)	73(5)	37(5)
	r2	0.110(2)	108(12)	49(13)	125(14)	0.121(2)	107(14)	69(13)	140(12)	0.136(2)	87(23)	23(22)	112(17)
	r3	0.116(2)	34(8)	57(9)	95(8)	0.126(2)	146(10)	124(9)	73(13)	0.139(2)	47(5)	75(31)	63(15)
T2	r1	0.106(2)	45(9)	125(5)	79(16)	0.114(2)	52(7)	131(4)	76(13)	0.117(3)	131(4)	77(5)	28(5)
	r2	0.110(2)	68(13)	101(10)	167(15)	0.120(2)	65(9)	102(9)	165(13)	0.136(2)	114(6)	46(7)	117(6)
	r3	0.126(2)	53(4)	37(3)	96(4)	0.141(2)	48(3)	44(3)	93(3)	0.149(2)	50(5)	47(7)	81(5)
M1	r1	0.118(3)	95(7)	90	12(7)	0.132(3)	82(9)	90	25(9)	0.135(5)	118(8)	90	11(8)
	r2	0.129(3)	90	180	90	0.141(3)	90	180	90	0.156(4)	90	180	90
	r3	0.135(3)	5(7)	90	102(7)	0.147(3)	172(9)	90	65(9)	0.161(4)	28(8)	90	79(8)
M2	r1	0.130(3)	71(13)	90	35(13)	0.139(3)	78(8)	90	28(8)	0.148(4)	117(14)	90	10(14)
	r2	0.133(3)	90	180	90	0.149(3)	90	180	90	0.159(4)	90	180	90
	r3	0.139(3)	161(13)	90	55(13)	0.154(3)	169(8)	90	62(8)	0.161(4)	26(15)	90	81(5)
M3	r1	0.114(4)	127(7)	90	20(7)	0.120(4)	129(5)	90	22(5)	0.119(7)	138(5)	90	31(5)
	r2	0.115(4)	90	180	90	0.135(4)	90	180	90	0.148(6)	90	180	90
	r3	0.138(4)	37(7)	90	70(7)	0.159(4)	39(5)	90	68(5)	0.175(5)	48(5)	90	59(5)
M4	r1	0.137(2)	69(1)	90	38(1)	0.152(2)	68(1)	90	38(1)	0.168(4)	72(1)	90	35(1)
	r2	0.153(2)	90	180	90	0.166(2)	90	180	90	0.179(3)	90	180	90
	r3	0.242(2)	159(1)	90	52(1)	0.269(2)	158(1)	90	52(1)	0.277(3)	162(1)	90	55(1)
A	r1	0.187(10)	57(5)	80(13)	51(6)	0.199(22)	56(6)	73(11)	55(9)	0.220(17)	61(8)	82(7)	47(8)
	r2	0.259(23)	79(10)	22(10)	111(11)	0.298(23)	69(7)	40(11)	128(13)	0.378(34)	74(19)	25(20)	113(16)
	r3	0.412(23)	145(5)	71(8)	47(6)	0.464(45)	138(6)	55(8)	58(7)	0.444(34)	146(12)	67(21)	51(12)

a Error in parentheses represents one standard deviation.

Table A10. Unit cell parameters of richterites

	K fluor-richterite				Na fluor-richterite				
	24°C	400°C	600°C	800°	24°C	400°C	600°C	800°C	900°C
I2/m cell									
a(Å)	9.992(1)a	10.041(1)	10.070(1)	10.104(1)	9.938(2)	9.979(2)	10.008(2)	10.032(1)	10.043(1)
b(Å)	17.972(3)	18.056(2)	18.106(2)	18.159(2)	17.952(4)	18.036(3)	18.087(2)	18.131(2)	18.149(1)
c(Å)	5.260(1)	5.272(1)	5.278(1)	5.285(1)	5.258(1)	5.270(1)	5.278(1)	5.284(1)	5.286(1)
β(°)	105.80(1)	105.83(1)	105.83(1)	105.85(1)	106.62(1)	106.71(1)	106.69(1)	106.70(1)	106.69(1)
V(Å³)	908.9(2)	919.7(2)	925.9(2)	933.0(2)	899.0(3)	908.4(3)	915.2(4)	920.6(2)	923.0(2)
asinβ(°)	9.614	9.661	9.688	6.720	9.523	9.557	9.587	9.609	9.620
C2/m cellb									
a(Å)	9.944	9.987	10.013	10.043	9.824	9.855	9.883	9.904	9.915
b(Å)	17.972	18.056	18.106	18.159	17.952	18.036	18.087	18.131	18.149
c(Å)	5.260	5.272	5.278	5.285	5.258	5.270	5.278	5.284	5.286
β(°)	104.79	104.70	104.64	104.57	104.22	104.11	104.07	104.02	104.01

a Error in parentheses is one standard deviation.
b All parameters for C cell calculated from those of the I-cell.